

Roger Miró Serra

**Hydrocinnamaldehyde production by Rh-catalysed
regioselective hydroformylation of styrene.**

FINAL DEGREE PROJECT

Supervised by Dr. Cyril Godard

Chemistry degree



UNIVERSITAT ROVIRA I VIRGILI

Tarragona

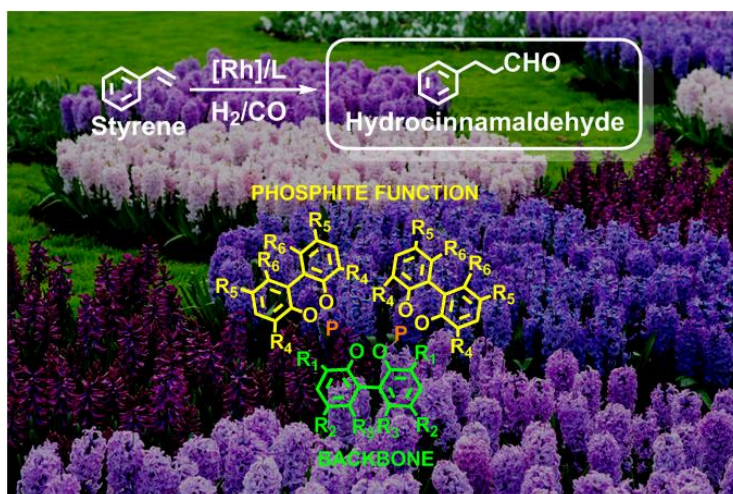
2018

Index

1. Abstract.....	4
2. Introduction	5
2.1. Industrial applications of hydroformylation: Fragrances	6
2.2. Rh-catalysed hydroformylation mechanism	7
2.3. Rhodium catalysed styrene hydroformylation: the regioselectivity issue	9
2.4. Large natural bite angles ligands	11
2.4.1. Xantphos derivatives.....	11
2.4.2. Calixarene-based diphosphites	13
2.5. Atropoisomeric bidentate ligands.....	14
2.5.1. Tetrakisphosphorus binol-based Ligands	14
2.5.2. Bidentate binaphthol based ligands.....	16
3. Objectives	18
4. Results and discussions.....	19
4.1 Synthesis of new atropoisomeric backbones	19
4.1.1 Reduction step	19
4.1.2 Coupling step	19
4.1.2.1 Cross dehydrogenative coupling step	20
4.1.2.1.1 Approach 1.....	20
4.1.2.1.2 Approach 2.....	20
4.1.2.1.3 Approach 3.....	22
4.1.2.2 Alternative approach: Suzuki-Miyaura cross-coupling.....	25
4.1.2.2.1 Bromination step	26
4.1.2.2.2 Alcohol silylation step.....	26
4.2. Synthesis of new diphosphite ligands	27
4.2.1. Synthesis of diphosphite L1	28
4.2.2. Synthesis of diphosphite L5	29
4.2.3. Synthesis of diphosphite L2	30
4.2.4. Synthesis of diphosphite L6	31
4.3. Rh-catalysed hydroformylation of styrene	32
5. Conclusions.	35
6. Experimental part.....	36
7. References.....	41
8. Supporting information: NMR spectra of products and intermediates	44

1. Abstract

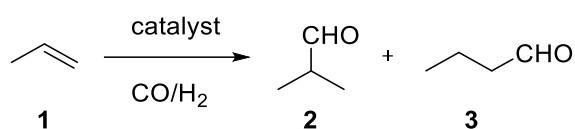
Hydrocinnamaldehyde and hydrocinnamyl alcohol (a derivative produced by hydrogenation of hydrocinnamaldehyde) are interesting compounds for the industrial production of floral fragrances because of its powerful hyacinth aroma and sweet and floral odour, respectively. These compounds are currently produced by selective or full hydrogenation of cinnamaldehyde, although the regioselective Rh-catalysed hydroformylation of styrene has recently emerged as an interesting alternative for the preparation of hydrocinnamaldehyde. The work presented here deals with the design and preparation of diphosphite ligands for their application in the linear regioselective Rh-catalysed hydroformylation of styrene. The catalytic performance of the catalysts was affected by the structures of the diphosphite backbone and phosphite function (Scheme 1).



Scheme 1. Hydrocinnamaldehyde production by Rh-diphosphite reverse regioselective hydroformylation of styrene.

2. Introduction

In 1938, Otto Roelen¹ discovered the hydroformylation of alkenes that is nowadays one of the most important industrial applications of homogeneous catalysis (Scheme 2).^{2,3} Today, over 9 million tons of so-called oxo-products are produced for year, a number still increasing. These oxo-products are mainly obtained from hydroformylation of propene **1**, which is a fraction of the steam-cracking process. The resulting products *iso*-butyraldehyde **2** and *n*-butanal **3** are important intermediates for the production of esters, acrylates and 2-ethylhexanol.²



Scheme 2. Hydroformylation of propene.

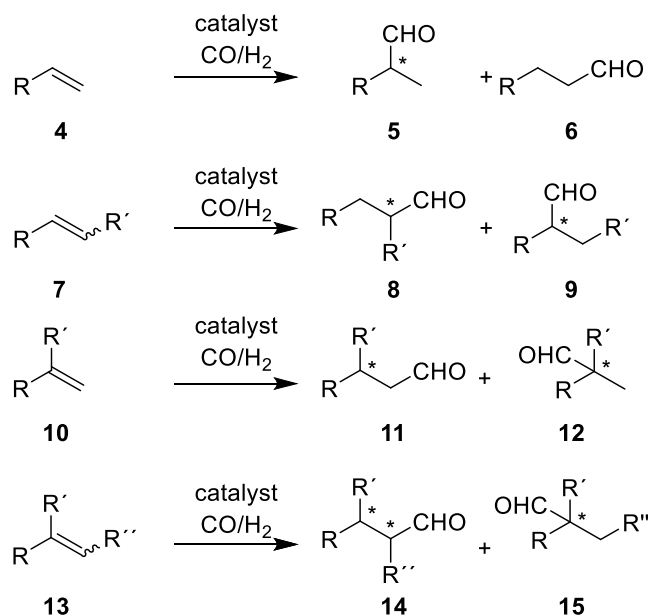
The hydroformylation reaction, from a synthetic point of view is a one-carbon chain elongation caused by the addition of carbon monoxide and hydrogen across the π system of a C=C double bond.^{4,5} The hydroformylation introduces an aldehyde function which permits the skeleton expansion and this reaction meets all requirements of an atom economic process.^{6,7}

The first generation of hydroformylation catalysts was based on cobalt. However, in 1968, Wilkinson reported the use of rhodium complexes modified with phosphine ligands in this reaction, providing a significantly higher activity and selectivity than the first generation of cobalt catalysts.⁸ Since this discovery, in order to influence the catalyst activity and selectivity the method of choice was the ligand modification of the rhodium catalyst.⁹

Strong π -acceptor ligands, for example bulky phosphites and phosphobenzene systems are used in hydroformylation catalysis.¹⁰ However, the rhodium catalysts have a high activity and is usually associated with a high tendency towards alkene isomerisation, therefore a selective hydroformylation of an internal alkene remains a challenge, even though in the last years some examples started to appear in the literature.

One of the problems to be solved in industry is the chemoselectivity and regioselectivity in low-pressure hydroformylation of internal alkenes. This problem originates from the exponential drop of alkene reactivity when increasing the number of alkene substituents.

There are many factors that influence the regioselectivity of the hydroformylation of alkenes,¹¹ for example, the inherent substrate preferences, directing effects exerted by functional groups as part of the substrate, as well as catalyst effects. To appreciate the substrate regioselectivity trends, the alkenes are classified according to the number and nature of their substituents (Scheme 3).^{4,5}



Scheme 3. Regioselective trends on hydroformylation of different alkenes.

The regioselectivity problem is usually related to terminal and 1,2-disubstituted alkenes **7**. The linear product **6** is preferably formed from alkyl-substituted terminal alkenes **4**. The branched product **5** is favoured from terminal alkenes **4** containing an electron-withdrawing substituent. Both 1,1-disubstituted **10** and trisubstituted **13** alkenes generally provide only one regioisomer (**11** and **14**, respectively).¹²

2.1. Industrial applications of hydroformylation: Fragrances

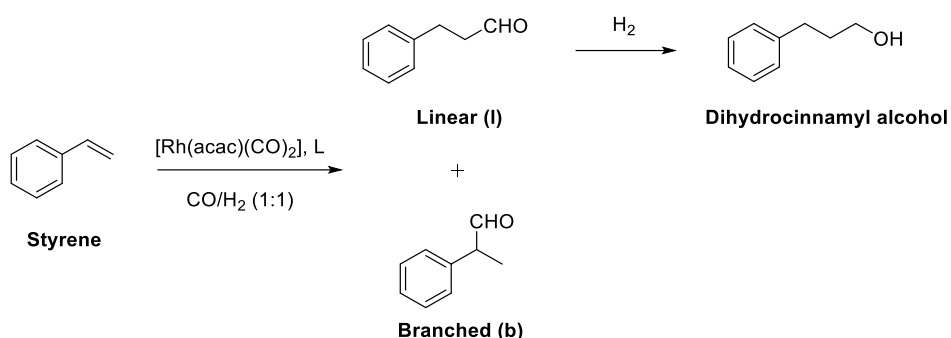
The homogeneous hydroformylation reaction is one of most attractive synthetic methods for the production of aldehydes, acetals, and alcohols. These compounds are used as ingredients in numerous perfumes, flavours and foodstuffs due to its aroma.¹³

Historically, the only way to obtain these aroma products was from natural products, such as extraction from plants and recovery from mostly rare animals. The industrial production of fragrances started at the end of the 19th Century and these developments was stimulated by the high costs of the natural products and the increasing demands for larger amounts of these compounds for use in cosmetics, air fresheners, detergents, cleaning agents and as food additives.

The worldwide production scale of flavours and fragrances is close to that of the pharmaceutical industry, whereas the scale prices are closer to the bulk chemicals. In 2017, the total market for flavours and fragrances had an estimated value of 26.300 million USD and about three quarters of the total volume was achieved by only ten companies.^{14,15}

For the hydroformylation chemistry to obtain fragrances is a crucial prerequisite ensure a high chemo- and regioselectivity, because small amounts of by-products can contaminate the desired odour. In asymmetric hydroformylation reactions, almost-complete enantioselectivity is desired, although naturally occurring compounds (e.g., some terpenes) may also not be completely enantiomerically pure.¹⁶

In the case of the hydroformylation of the styrene, the linear aldehyde **I** (Scheme 4) product has a powerful hyacinth aroma for floral fragrances. Hydrogenation of the linear aldehyde provides dihydrocinnamyl alcohol, which has a sweet and floral odour. Until now, the dihydrocinnamyl alcohol is usually prepared by hydrogenation of cinnamaldehyde.¹³

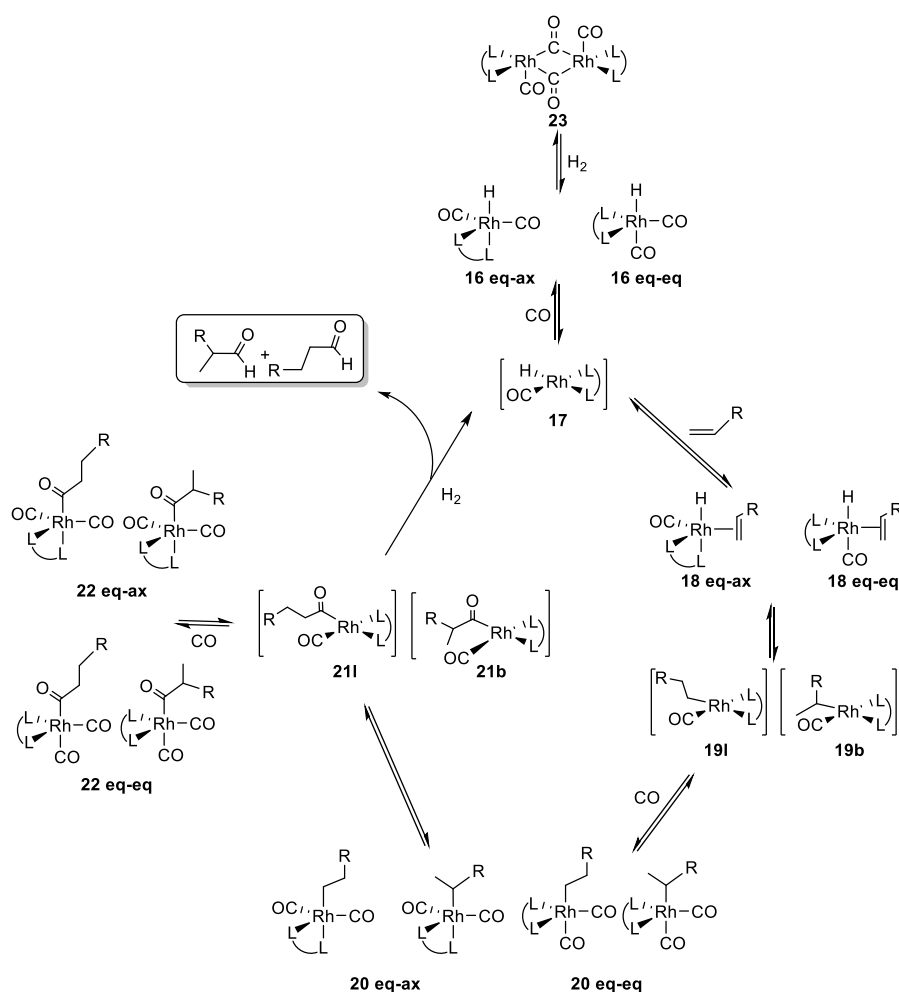


Scheme 4. Industrial application of the hydroformylation of styrene.

2.2. Rh-catalysed hydroformylation mechanism

In Scheme 5, the Rh-catalysed hydroformylation dissociative mechanism is described for bidentate ligands.¹⁷ The associative mechanism involving 20-electron intermediate for ligand/substrate exchange is not considered.⁸ A great understanding of this process mechanism has been possible thanks to high pressure spectroscopic techniques (HP-IR, HP-NMR) which allow the in situ observation and structural characterisation of the resting state of the catalyst.^{9,18} The common starting complex for bidentate ligands (L-L) is the [RhH(L-L)(CO)₂] specie **16**, which can contain the ligand coordinated in equatorial positions (indicated as eq-eq, Scheme 5) or in an axial-equatorial positions (indicated as eq-ax, Scheme 5). The dissociation of the equatorial CO from **16** leads to the square-planar intermediate **17**, which give the complexes **18** when associating with alkene, where the ligand can again be coordinated in two isomeric forms eq-ax and eq-eq. The experimental results and theoretical calculations indicate that the regioselectivity is determined by the coordination of the alkene to the intermediate **17** to form the intermediates **18**.¹⁹ The determination of the enantioselectivity is also taking place during this step since the enantioface discrimination occurs between **17** to **18**. The CO dissociation from **16** is much faster than the overall hydroformylation process, indicating that the rate determining step of

the reaction is the reaction of **17** with either CO or alkene to form **16** or **18**.²⁰ In Scheme 5, all the steps are described as reversible except the final hydrogenolysis, even though, the alkene complexation reversibility has not been established experimentally. Complexes **18** suffer migratory insertion to give the square-planar alkyl complex **19**. The species **19** can suffer a β -hydride elimination, thus leading to isomerisation, or can react with CO to form the bipyramidal complexes **20**. More isomerisation may be expected under low pressure of CO.



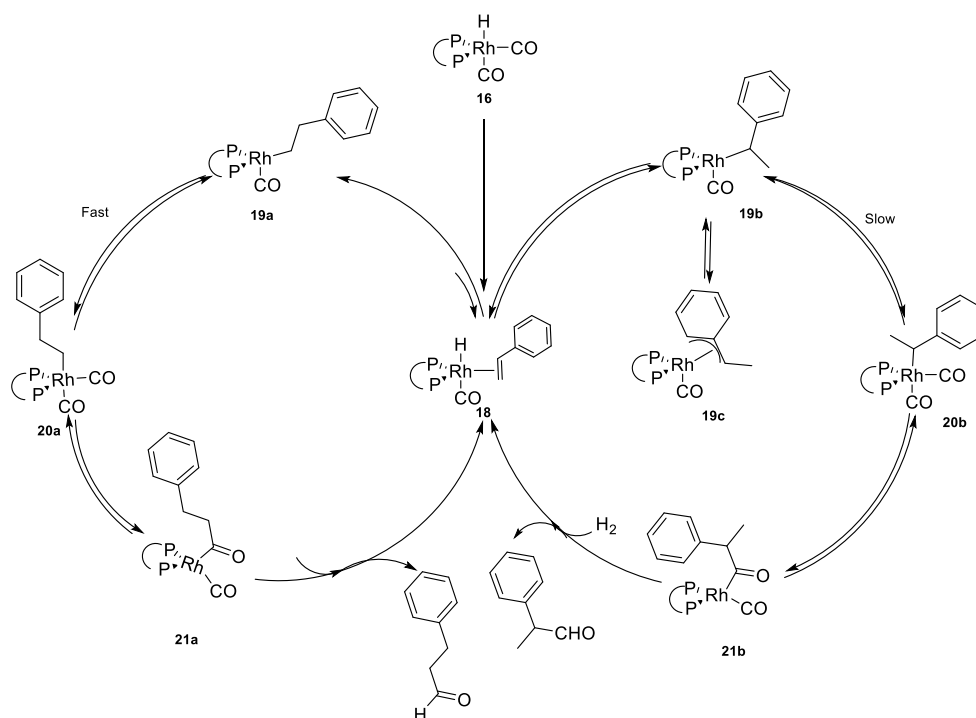
Scheme 5. Mechanism of the Rh-catalysed asymmetric hydroformylation in the presence of bidentate ligand (L-L).

At low temperatures (< 70°C) and a sufficiently high pressure of CO (> 10bar), the insertion reaction is usually irreversible and the regioselectivity and the enantioselectivity in the hydroformylation of alkenes is determined at this point. Complexes **20** suffer the second migratory insertion to form the acyl complex **21**, which can react with CO to give the saturated acyl intermediates **22** or with H₂ to give the aldehyde product and the intermediate **17**. The reaction with H₂ presumably involves an oxidative addition and reductive elimination, but for rhodium no trivalent intermediates have been observed.²¹

2.3. Rhodium catalysed styrene hydroformylation: the regioselectivity issue

The transformation of styrene into the corresponding aldehydes has been largely reported.²² As previously mentioned, for the terminal alkenes **4** (Scheme 3) containing an electron-withdrawing substituent, the formation of the branched product **5** is favoured.

The mechanism of the rhodium catalysed hydroformylation of styrene has been studied in depth.²³ The proposed catalytic cycle is shown in Scheme 6.



Scheme 6. Proposed mechanism for the Rh-catalysed hydroformylation of styrene.

In this mechanism, the key step to control the regioselectivity is the formation of the rhodium alkyl intermediates **20a** and **20b** from the Rh hydride species **18**. Lazzaroni and co-workers showed that the kinetic product is the branched aldehyde and is favoured when the reaction is performed at low temperature. The branched product is favoured for the formation of the stable Rh(η^3 -allyl) species **19c**, which is in equilibrium with the branched Rh-alkyl species **19b**. The presence of this species tends to displace the equilibrium towards the catalytic cycle giving rise to the branched product.

In these studies, the effect of the temperature was shown to affect the regioselectivity of this process and demonstrated that the formation of both linear and branched Rh-alkyl species is irreversible at low temperature but becomes reversible at high temperature.²³

Brown and Kent reported that the coordination mode of the phosphine ligands could also influence the regioselectivity of the reaction: the steric hindrance provided by de eq-eq

coordination favours the formation of the linear product but the eq-ax coordination of the ligand favours the formation of the branched product.²⁴

There are only few examples in the literature concerning the selective formation of the linear aldehyde in the hydroformylation of styrene. In the following sections, the most relevant systems providing the regioselective linear hydroformylation of the styrene will be described according to the types of ligands used: presenting large natural bite angles and presenting atropisomeric backbone (Figure 1).

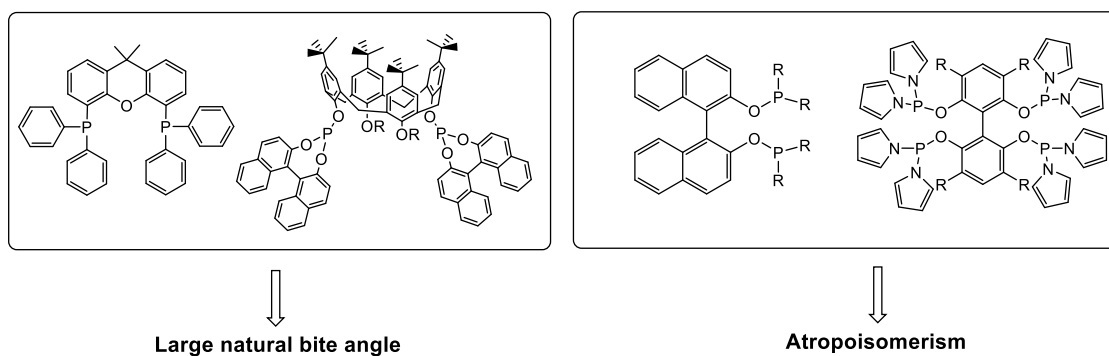


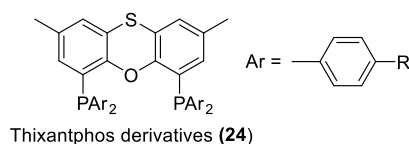
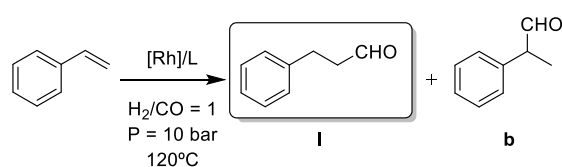
Figure 1. Ligands reported to provide high linear regioselectivity in the Rh-catalysed hydroformylation of styrene.

2.4. Large natural bite angles ligands

2.4.1. Xantphos derivatives

The research group of van Leeuwen and co-workers studied the effect of diphosphine ligands on the activity and regioselectivity of Rh-catalysts in the hydroformylation of alkenes using large natural bite angle ligands.^{25,26}

In 1998, these authors reported a study on the electronic effect in the Rh diphosphine catalysed hydroformylation of alkene using a series of thixantphos ligands **24** (Scheme 7) varying the groups in *para* position of the phenyl substituents at phosphorus using various electron donating and electron withdrawing groups.²⁷



R	l/b ratio	TOF
NMe ₂	0.75	1100
OMe	0.85	1800
Me	1.1	2800
H	1.3	3100
F	1.3	2900
Cl	1.4	3200
CF ₃	1.8	3400

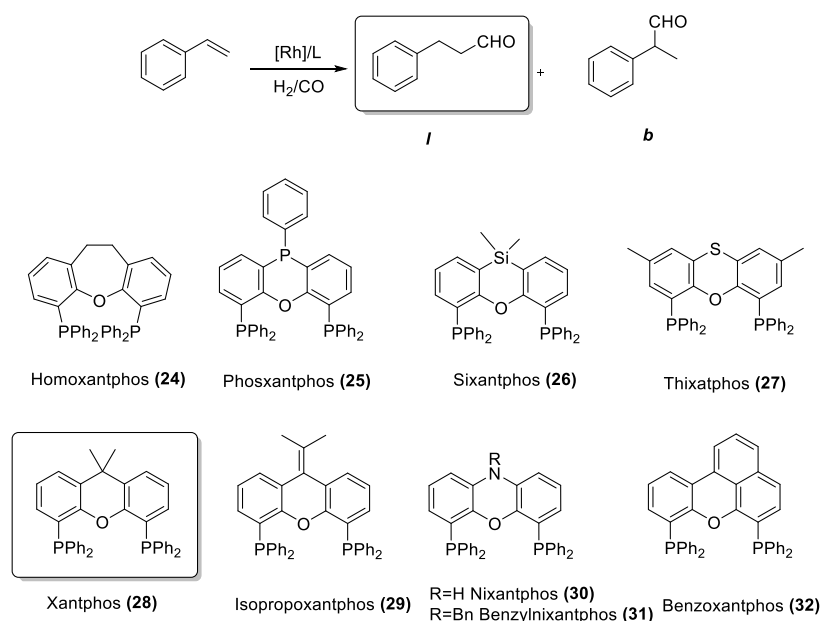
Scheme 7. Electronic effect in Rh-catalysed hydroformylation of styrene using thixantphos ligands.

An increase in l/b ratio and activity was observed in the hydroformylation of the styrene with decreasing phosphine basicity (Scheme 7) while a pronounced effect of phosphine basicity on the chelation mode of the ligands in the (diphosphine)Rh(CO)₂H complexes was observed. The ee:ea isomer ratio, observed in the IR and NMR spectra, showed a regular increase with decreasing phosphine basicity. The spectroscopic results were supported by theoretical calculations using DFT. The electronic ligand effect on catalysis is reflected in both hydroformylation rate and rate of β -hydrogen elimination.

To investigate the exact correlation between the selectivity and the natural bite angle of diphosphine ligands in the rhodium catalysed hydroformylation of styrene, the same group developed a new family of ligands based on xanthene backbone and hypothesised an increase in selectivity to linear aldehyde with the increase of the natural bite angle.²⁸ In this

study, the styrene hydroformylation process was carried out at 120°C and 10 bar of 1:1 CO/H₂ using a 0.5 mM solution of rhodium precatalyst and 10 equivalents of ligand. These reaction conditions were previously reported to enhance the l/b ratio in this reaction. The results of this work are summarised in Table 1.

Table 1. Rh-catalysed hydroformylation of styrene using Xantphos derivatives.



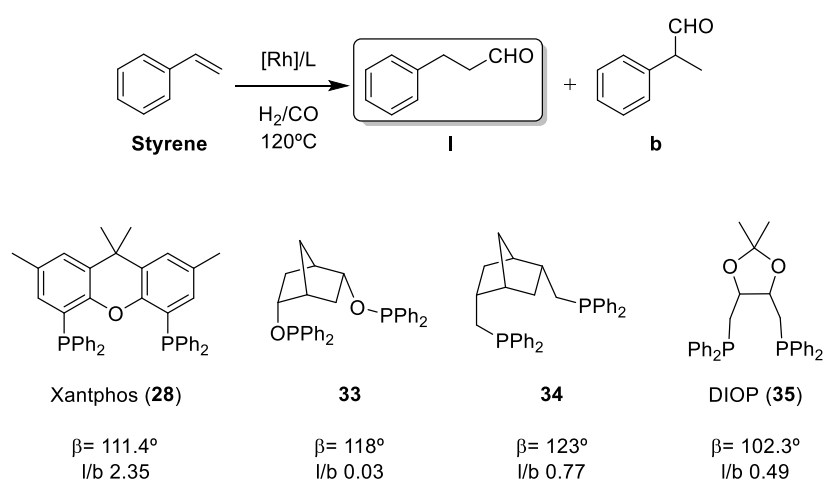
Entry	Ligand	Bite angle	l/b ratio	Linear RCHO (%)
1	24	102 °	0.68	40
2	25	107.9 °	1.13	53
3	26	108.5 °	0.99	50
4	27	109.6 °	1.22	55
5	28	111.4 °	1.45	59
6	29	113.2 °	1.45	59
7	30	114.1 °	1.78	64
8	31	114.2 °	2.04	67
9	32	120.6 °	1.78	64

Reaction conditions: [Rh(acac)(CO)₂] (0.5 mM); Ligand/Rh (10); Styrene/Rh (1746); CO/H₂ (1:1, 10 Bar); toluene (8.5 mL); 12h

Within this series, the highest selectivity was obtained with ligand **31** (67%, Entry 8, Table 1). When the bite angle was increased from 102° to 114°, an increase in linear to branched ratio (Entry 1-8, Table 1) was clearly observed. However, when ligand **32**, which exhibits a natural bite angle of 120°, was used, the selectivity slightly decreased.

In this study, the authors concluded that the natural bite angle of the ligands correlates well with the selectivity for linear aldehyde in the hydroformylation of styrene due to a higher congestion around the metal centre. However, no clear correlation between the natural bite angle and the eq-eq/eq-ax isomer ratio was observed.

The same research group later demonstrated that the rigidity of the ligand backbone is also an important factor analysing the effect of the structure of the ligand backbone on the selectivity of the Rh-catalysed hydroformylation.²⁸ Indeed, comparing results obtained with a series of bidentate ligand presenting large natural bite angles (Scheme 8), they showed that a rigid backbone such as Xantphos (**28**) provides the highest l/b ratio in this process.

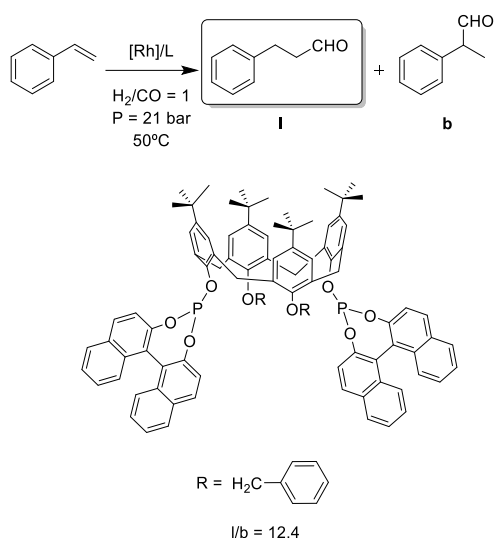


Scheme 8. Rh-catalysed regioselective styrene hydroformylation.

In summary, the works developed by the group of van Leeuwen showed that large bite angle diphosphine ligands provide high regioselectivity in the Rh-catalysed hydroformylation of alkenes to the linear aldehyde products. However, the effect of the natural bite angle remain unclear since the basicity and rigidity of the backbone were also shown to affect the regioselectivity of this process. Furthermore, theoretical calculations indicated that interactions between the aromatic substituents at phosphorus were playing a central role in governing the regioselectivity and that the bite angle effect was less important.

2.4.2. Calixarene-based diphosphites

In 2010, Semeril and co-workers studied the effect of calixarene-based diphosphite ligands on the activity and regioselectivity of Rh-catalysts in the hydroformylation of styrene.²⁹



Scheme 9. Calixarene-based diphosphites reported by Semeril and co-workers.

Semeril and co-workers took advantage of the large bite angle of calixarenes based diphosphite ligands (Scheme 9) for rhodium catalysed styrene hydroformylation process, in order to obtain high linear to branched ratio. In this study, the reaction was carried out at 50°C and 21 bar of 1:1 CO/H₂ using a 2 μmol solution of rhodium precatalyst.

The result of this work is the 12.4 linear to branched ratio in styrene hydroformylation. A calixarene is a macrocycle or cyclic oligomer based on a hydroxyalkylation product of a phenol and an aldehyde. Calix[4]arenes are formed by 4 units and the internal volume of the ring is around 10 cubic angstroms. Calixarenes are characterised by a wide upper rim and a narrow lower rim and a central annulus. The 4 hydroxyl groups interact by hydrogen bonding and stabilise the cone conformation. This conformation is in dynamic equilibrium with the other conformations.

2.5. Atroposiomeric bidentate ligands

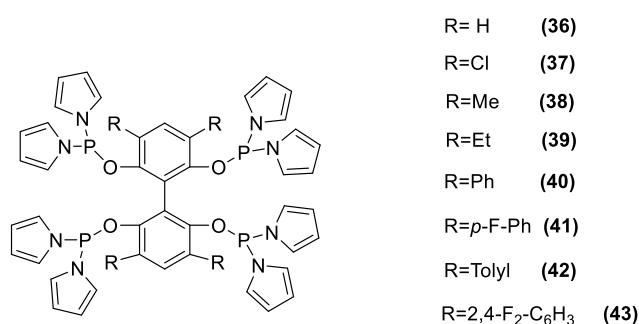
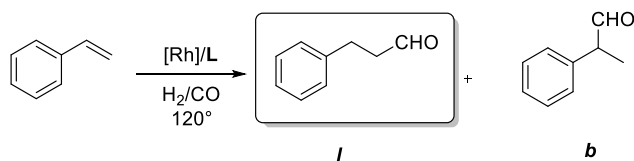
2.5.1. Tetraphosphorus binol-based Ligands

Another important family of ligands for highly regioselective hydroformylation is the bulky tetraphosphorus ligands developed by Zhang and co-workers.³⁰ These tetraphosphorus ligands are able to chelate the metal in four different modes. In addition, when the ligand coordinates with the metal, the remaining two phosphorus atoms increase the local phosphorus concentration around the metal centre. The electronic effects of ligands on the catalyst activity and regioselectivity were studied by changing the substituent at *para* position of the phenyl group from strong electron-donating groups to strong electron-

withdrawing groups. In order to understand better the behaviour of the substituent on the regioselectivity of styrene hydroformylation.

Based on the best condition found out for ligand **36** (Entry 1, Table 2) they decided to test different moieties on the ligand backbone. It was found that the introduction of substituents on the 3,3'-5,5' position of the biphenyl moiety greatly increased the regioselectivity for the linear aldehyde as shown in Table 2.

Table 2. Styrene hydroformylation with tetra phosphorous derivatives^a.



Entry ^a	Ligand	Conv %	I/b ratio	% Linear aldehyde
1	36	80	6.8	87
2	37	98	12.9	92.8
3	38	71	15.9	94.1
4	39	54	17.2	94.5
5	40	99	19.3	95.1
6	41	99	20.3	95.3
7	42	95	22.4	95.7
8 ^b	43	89	26	96.3

Reaction conditions: ^a[Rh(acac)(CO)₂](1 μmol), Ligand (3 μmol), Styrene (10 mmol), CO/H₂ (1:1, 5 atm), Temperature 80° C, toluene (4.9 mL); ^bligand/Rh ratio= 4.

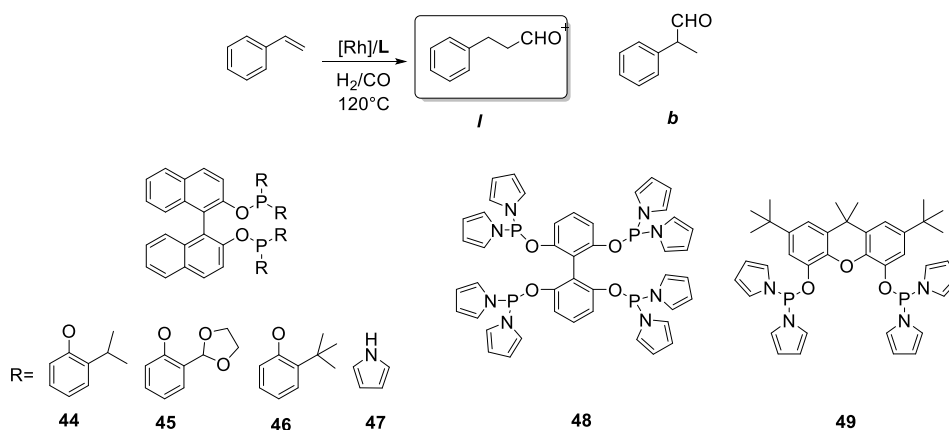
Zhang and co-workers reported the results about the styrene hydroformylation process that was carried out at 80°C and 10 bar of 1:1 CO/H₂ using a 1.0 mM solution of Rh precatalyst and 3 equivalents of ligand. The use of ligand **37** (Entry 2, Table 2) bearing a chloride substituent increased the linear to branched ratio from 6.8 to 12.9 when compared with the unsubstituted ligand. Similar results with the alkyl substituted ligands **38** and **39** (Entry 3,4, Table 2) although in these latter cases, the conversion dropped significantly. These results

clearly indicated that an increase in steric bulk favours the regioselectivity of the reaction towards the linear aldehyde while the electronic properties of the ligand mainly affect the catalytic activity. Further increase in steric hindrance of the ligands by introduction of aryl substituents (Entries 5-8, Table 2) provided l/b ratios up to 26. The difference observed between the catalytic performance of **42** and **43** was attributed to an electronic effect since similar steric hindrance is expected for both ligands. They concluded that for two ligands exhibiting similar steric hindrance, the presence of electron withdrawing groups like in **43** favours the formation of the linear aldehyde.

2.5.2. Bidentate binaphthol based ligands

Binaphthol based ligands have been applied in various homogeneous catalytic reactions.³¹ In 2013, Vogt and co-workers compared the catalytic performance of a series of Rh catalysts bearing various bidentate ligands: four binaphthol based ligands, one xantphos derivative and a tetraphosphorus ligand (Table 3).³²

Table 3. Rh-catalysed hydroformylation of styrene using binaphthol derivatives and phosphorodiamidite based ligands.

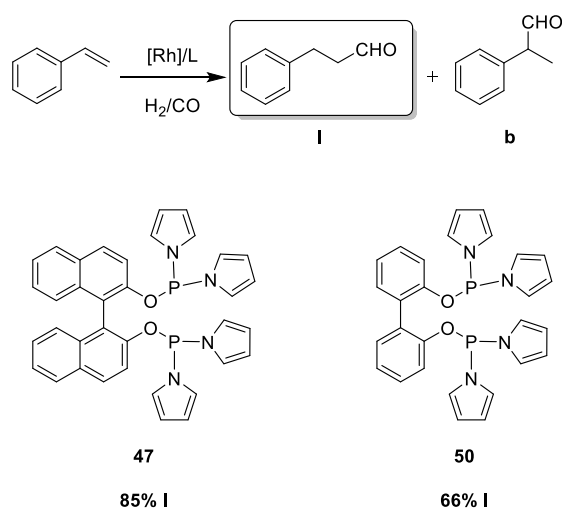


Entry	Ligand	T (°C)	l/b ratio	% Linear aldehyde
1	44	80	0.37	27
2	45	80	0.97	49
3	45	140	7.1	88
4	46	80	-	-
5	47	80	4.9	83
6	48	80	5.8	85
7	49	80	2.5	71

Reaction conditions: [Rh] (1 eq, 14 μ mol), Rh precursor [Rh(acac)(CO)₂], Ligand (2 eq, 28 μ mol), Styrene (2000 eq, 28.8 mmol), CO/H₂ (1:1, 10 bar), Solvent (5 ml).

Comparing the binaphthol based ligands **44**, **45** and **47** (Entry 1, 2 and 5 respectively, Table 3) showed good activity, while **46** (Entry 4, Table 3) did not provide any conversion. The absence of activity in the latter was attributed to the steric hindrance induced by the tert-butyl groups in *ortho* position of the phenoxy moiety on the ligand. When the reaction was performed with ligand **45** at 140°C (Entry 3, Table 3), an increase in linear to branched ratio up to 7.1 was observed, although more hydrogenation was also detected. The highest regioselectivities at 80°C were obtained with the pyrrole substituted ligands **47**, **48** and **49** (Entry 5, 6 and 7 respectively, Table 3), indicating that ligands with more pronounced π acceptor properties favour the linear product under these conditions.

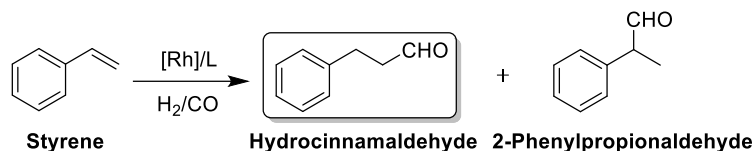
In 2013, Zhang and co-workers compared a series of ligands with different backbones and substituents.³³ Eight different ligand backbones were tested under the same conditions and the ligand that contains the pyrrole moiety showed better performance in terms of regioselectivity to linear aldehyde. The binaphthol based ligand **47** (see Scheme 10) provided the highest regioselectivity with 85% of linear aldehyde. Interestingly, the ligand **50**, which presents structural properties related to those of **47**, provided much lower selectivity to the linear aldehyde under the same conditions, indicating that the atropisomeric backbone is key to reach high selectivity in this reaction.



Scheme 10. Comparison of the results reported by Zhang on the Rh-catalysed hydroformylation of styrene using binaphthol and binol-based ligands.

3. Objectives

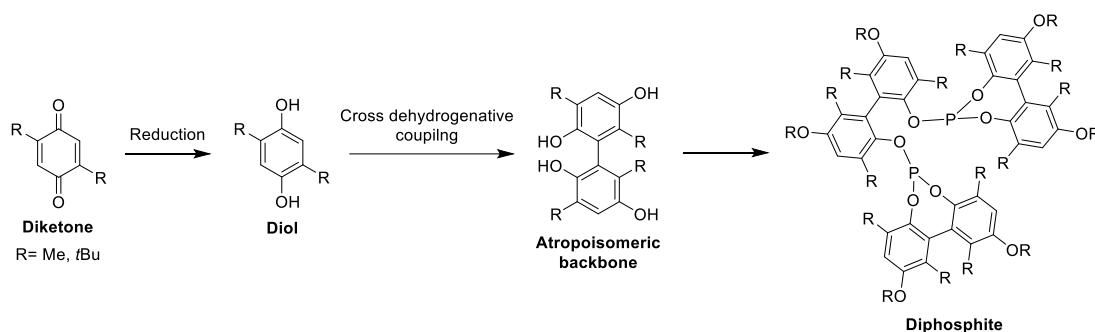
The main objective of this work is the hydrocinnamaldehyde production by Rh-diphosphite reverse regioselective hydroformylation of styrene.



Scheme 11. Rh-catalysed hydroformylation of styrene.

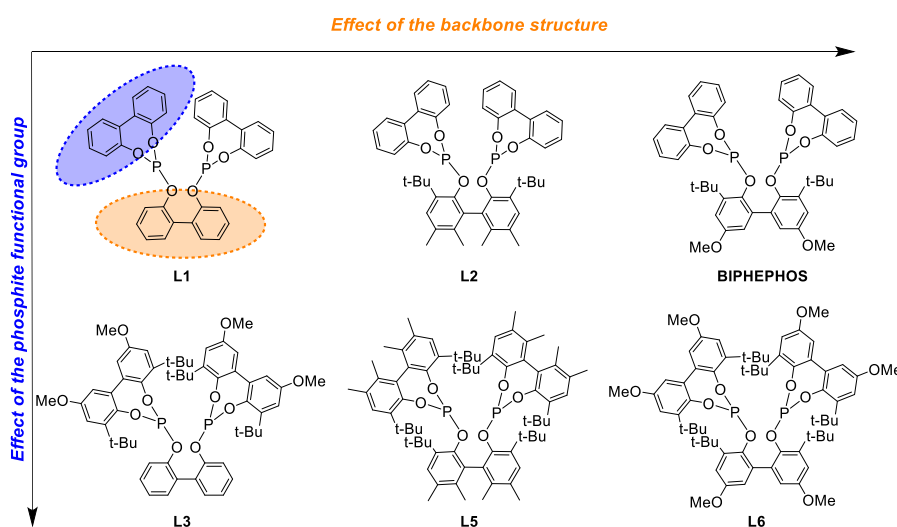
The partial objectives are:

1. Synthesis of new atropisomeric backbones. These atropisomeric backbones are proposed because of the high regioselectivity obtained with ligands presented in Table 2 and Table 3. The general strategy for the preparation of the compounds with atropisomeric backbone is presented in Scheme 12.



Scheme 12. General scheme of the proposed synthetic routes.

2. Synthesis of new diphosphite ligands. Variation of the diphosphite function and backbone.



Scheme 13. Proposed structure of diphosphites related to BIPHEPHOS structure.

3. Evaluation of these ligands in the Rh-catalysed hydroformylation of styrene.

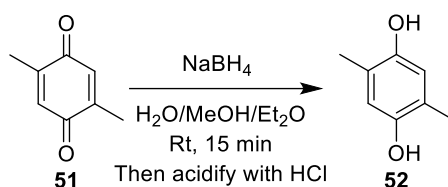
4. Results and discussions

4.1 Synthesis of new atropisomeric backbones

The synthesis of the atropisomeric backbones consisted in the reduction of commercially available 1,4-diketones and further coupling of this compounds to obtain a biphenol (see Scheme 12).

4.1.1 Reduction step

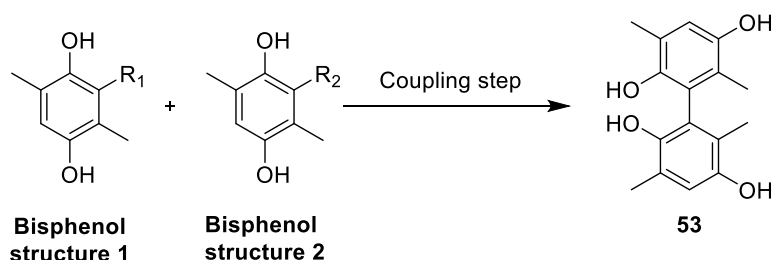
The first step of the ligands synthesis was the reduction of compound **51** into compound **52** with NaBH_4 by using adapted literature procedures.³⁴ The reaction proceeded smoothly at room temperature with excellent yield (92%). The compound **52** was previously described in the literature and NMR characterisation details corroborated its structure.



Scheme 14. Reduction step.

4.1.2 Coupling step

The next step of the synthesis was the coupling reaction of compound **52** to obtain the coupled product **53**. To do this, various approaches to couple **bisphenol structure 1** with **bisphenol structure 2** were considered: cross dehydrogenative coupling, Suzuki-Miyaura cross-coupling, Ullman and Kumada cross-coupling.



Cross dehydrogenative coupling: $\text{R}_1, \text{R}_2 = \text{H}$
Suzuki-Miyaura cross-coupling: $\text{R}_1 = \text{Br}; \text{R}_2 = \text{B}(\text{OH})_2$
Ullman reaction: $\text{R}_1, \text{R}_2 = \text{Br}$
Kumada cross-coupling: $\text{R}_1 = \text{MgBr}; \text{R}_2 = \text{Br}$

Scheme 15. Second step: Coupling step.

4.1.2.1 Cross dehydrogenative coupling step

We started testing the cross dehydrogenative step. Different approaches were evaluated:

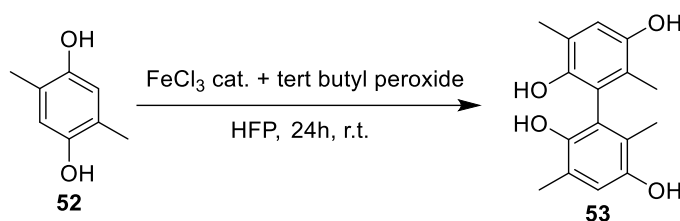
Approach 1, from the un-protected diol.

Approach 2, from the di-protected diol.

Approach 3, from the mono-protected diol.

4.1.2.1.1 Approach 1

In the approach 1 we evaluated the coupling of the un-protected compound **52** to obtain the coupled product **53**. To do this step we used FeCl_3 and an oxidant.



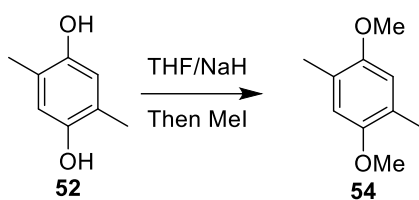
Scheme 16. Approach 1.

We performed the first test using FeCl_3 as catalyst, an oxidant (*tert*-Butyl peroxide) and 1,1,1,3,3,3-hexafluoro-2-propanol (HFP) as a solvent.³⁵ Using this route, we observed by ^1H NMR that the compound **52** was completely oxidised into the compound **51**. This is because the 1,4-hydroquinone reduces Fe(III) , generating semiquinone radicals that can oxidise Fe(II) back to Fe(III) .³⁶ We therefore carried out the same procedure using stoichiometric quantities of FeCl_3 as a softer oxidant agent. However, analysis by ^1H NMR revealed that the conversion was less than 5% and with the formation of a complex mixture of compounds. Since the cross dehydrogenative coupling of the un-protected diol **52** using catalytic or stoichiometric amounts of FeCl_3 were not effective, we decided to evaluate alternative procedures involving the protected diol to avoid its oxidation.

4.1.2.1.2 Approach 2

- **Di-protection of diol**

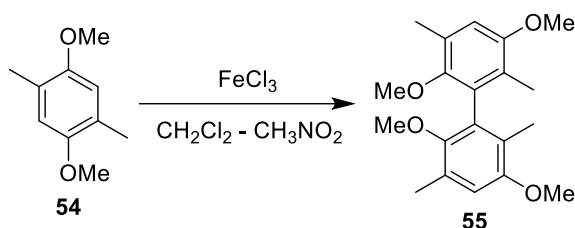
The first step of this new route was the protection of compound **52** to obtain compound **54**. This step was carried out by reacting diol **52** with an excess of NaH , and then, with MeI (Scheme 17).³⁷ After purification by flash chromatography the reaction product was isolated with moderate-to-high yields (68%). Since this compound was not reported in the literature, complete NMR characterisation was carried out to corroborate its structure.



Scheme 17. Di-protection of diol **52**.

We evaluated different procedures by variation of the oxidising agent and the use or not of a strong base to favour the de-protonation.

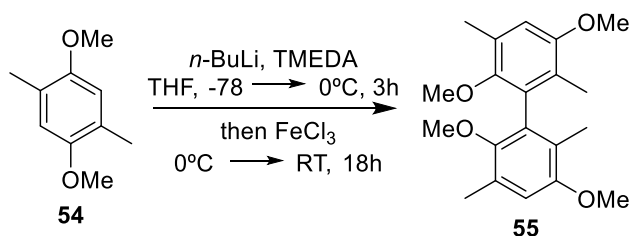
- **First procedure:** Soft oxidant agent.



Scheme 18. First procedure tested for the coupling from di-protected diol **54**.

This procedure involves the reaction of compound **54**, FeCl₃ (3 equivalents) and CH₂Cl₂ – CH₃NO₂ as a solvent mixture. The reaction was carried out at room temperature and for 24h following adapted procedures.³⁷ The reaction was monitored by TLC and ¹H NMR. After reaction, compound **54** was the only compound observed. In order to force the reaction to proceed we did the same reaction at higher temperature (reflux conditions). The results by ¹H NMR showed very low conversion (less than 5% was converted and with the formation a complex mixture of compounds). Our hypothesis was that the acidity of the protons involved in the coupling is much lower than those of the structures reported in the literature.³⁷

- **Second procedure:** soft oxidant + strong base.

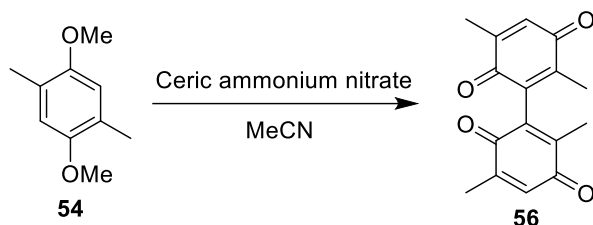


Scheme 19. Second procedure tested for the coupling from di-protected diol **54**.

Literature procedures described the use of *n*-BuLi as a base to favour the deprotonation of the aromatic compound during coupling processes.³⁸ This procedure involved the pre-treatment of compound **54** with *n*-BuLi (1.1 equivalents) and tetramethylethylenediamine (1.2 equivalents). At this point, the reaction mixture was reacted with FeCl₃ (1.2 equivalents). The

¹H NMR analysis showed less than 5% conversion with the formation a complex mixture of compounds. Even though a strong base was used, the coupled product **55** was not obtained.

- **Third procedure:** Strong oxidant agent.



*Scheme 20. Third procedure tested for the coupling from di-protected diol **54**.*

Since the oxidative coupling of the di-protected diol **54** using a weak oxidant (FeCl_3) was not efficient, we evaluated the use of ceric ammonium nitrate (CAN) (3.3 equivalents) which is a strong oxidant since literature reports described its efficiency for the coupling of similar backbones.³⁹ The results by ¹H NMR show that the compound **54** was completely oxidised to the compound **51** and we didn't have the product of coupling.

In conclusion, the cross dehydrogenative coupling of di-protected diol **54** was not proceeding under the evaluated reaction conditions probably due the difficulty of activating the aromatic protons with softer oxidant agent.

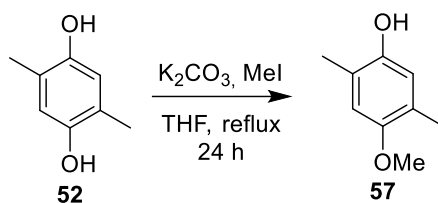
We did a new bibliographical search and found that the use of the mono-protected diol **57**, which takes advantage of the keto-enolic equilibrium and thus favours the activation of aromatic protons, could be an efficient alternative.

4.1.2.1.3 Approach 3

- **Mono-protection of diol**

The first step of this procedure of this new route involves the selective protection of compound **52** to obtain de mono-protected compound **57**. The selective mono-protection of the diol **52** is not straightforward step because the two alcohols are identical. Then, three selective mono-protection routes were evaluated:

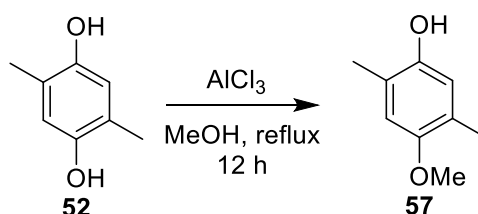
- **First procedure.**



*Scheme 21. First procedure tested for the mono-protection of diol **52**.*

Perform selective deprotonation by using a softer base than NaH, and then, methylation with MeI.⁴⁰ However, when this possibility was tested, no conversion was observed and we only recovered the compound **52**, maybe because the low solubility of K_2CO_3 in THF.

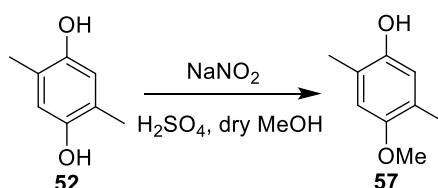
- **Second procedure.**



*Scheme 22. Second procedure tested for the mono-protection of diol **52**.*

We performed three tests of this procedure using 1.3, 2.0 and 2.7 equivalents of $AlCl_3$.⁴¹ Analysis of the results by 1H NMR revealed the presence in the final reaction mixture of three compound: unreacted compound **52**, mono-protected compound **57** and oxidation by-product **51** (1,4-dimethylbenzoquinone). The amount of $AlCl_3$ revealed crucial for controlling the ratio between product **57** and the product **51**. With 1.3 equivalents of $AlCl_3$ we observed 35% of conversion and 100% of selectivity to de compound **57**. With 2 equivalents of $AlCl_3$ there is 94% of conversion with 26% of selectivity to the compound **57** and appear the compound **51** (74% selectivity). With 2.7 equivalents there is 88% of conversion with 7% of selectivity to the compound **57** and 93% of selectivity to the compound **51**. Therefore, the sample obtained by using 1.3 equivalents of $AlCl_3$ was subjected to flash chromatography and the compound **57** was isolated in low yield (19%).

- **Third procedure.**



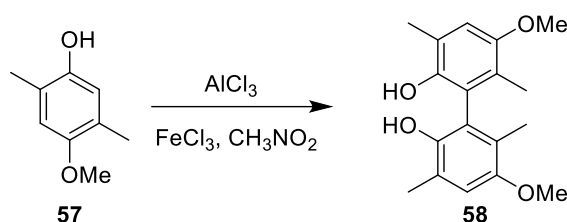
*Scheme 23. Third procedure tested for the mono-protection of diol **52**.*

We tested a third procedure reacting diol **52** with catalytic amounts of NaNO_2 under acidic conditions. Under acidic conditions, NaNO_2 forms HNO_2 in situ which rapidly decomposes forming NO_2 , which is capable of efficiently oxidise the hydroquinone to semiquinone radical that is easily esterified by reaction with alcohols in acidic medium.⁴²

After purification by flash chromatography the reaction product was isolated in high yield (92%). Since this compound was not reported in the literature, NMR characterisation was carried out to corroborate its structure.

- **Coupling using the mono-protected diol 57**

- **First procedure:** soft oxidant agent + strong Lewis acid.

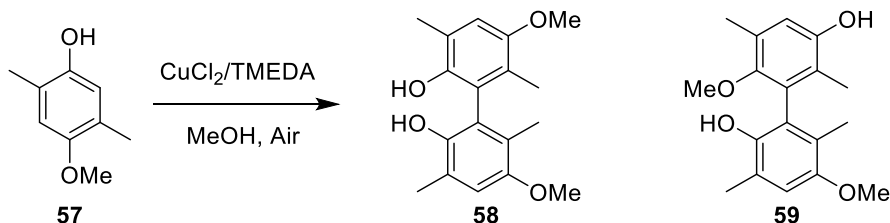


Scheme 24. First procedure tested for the coupling from mono-protected diol 57.

The first tested procedure consisted in reacting the compound **57**, AlCl_3 (1 equivalent) and FeCl_3 (1 equivalent) in dry CH_3NO_2 .⁴³ After stirring 6 hours at room temperature, the reaction was quenched with aqueous HCl solution (1M) and extracted with EtOAc . The results by ^1H NMR show that we only recovered the compound **57**.

Longer reaction times (12 and 24h) provided the same result. We therefore performed the reaction using 2 equivalents of FeCl_3 and the result by ^1H NMR show 60% of conversion with the formation of oxidation by-product **51** (1,4-dimethylbenzoquinone). The reaction was tested with temperature, 50 and 90°C , but we obtained a complex mixture of compounds.

- **Second procedure:** Cu-Catalyst + strong oxidant.

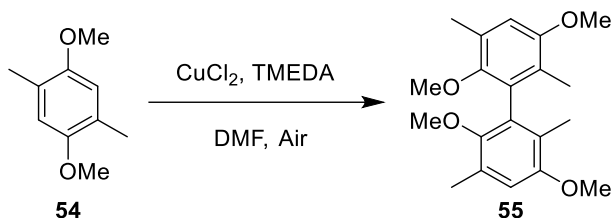


Scheme 25. Second procedure tested for the coupling from mono-protected diol 57.

The second procedure that we carried out involved the compound **57**, CuCl_2 ($6.25 \cdot 10^{-3}$ equivalents), N,N,N',N' -Tetramethylethylenediamine (TMEDA) ($9.375 \cdot 10^{-3}$ equivalents) and MeOH . This procedure was previously reported for the preparation of other biphenols (see Scheme 36).⁴⁴ After 24 hours under a continuous flow air, 70% conversion with the

formation of a complex mixture was obtained according to ^1H NMR. After flash chromatography, the product **59** was isolated in 17% yield.

Since this procedure provided a coupling product (although this product was not our target molecule), we thought that this procedure could be used for the coupling of compound **54** (di-protected diol) to obtain the product **55**.



*Scheme 26. Coupling from di-protected diol **54** using CuCl_2 .*

We carried out the reaction with the same conditions of the reaction with the mono-protected diol **57** but using DMF instead MeOH (due to the insolubility of **55** in MeOH). After 24h under continuous air flow, the work up was performed but ^1H NMR analysis showed that we had recovered the compound **54**.

In conclusion, the use of this synthetic route starting from the mono- or di-protected diols did not provide the desired products.

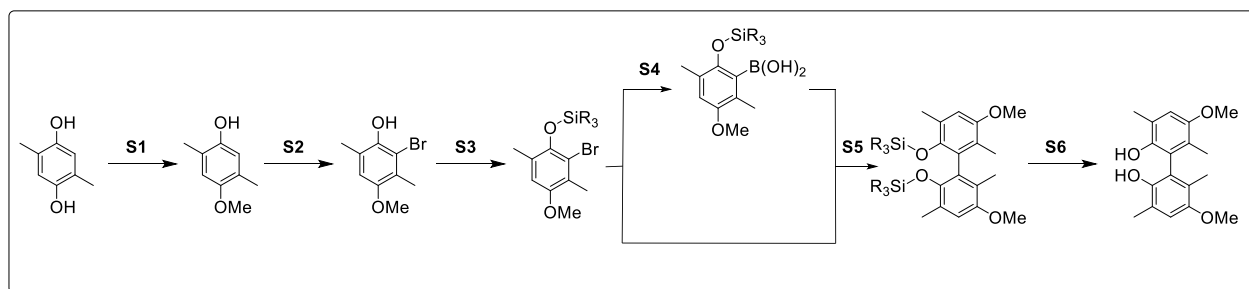
Because of all the approaches involving the cross dehydrogenative coupling were not successful and some of these procedures resulted in the formation of the starting benzoquinone by oxidation, we decided to evaluate procedures that do not involved this kind of reactivity, and then Suzuki-Miyaura cross-coupling was selected as a suitable procedure.

4.1.2.2 Alternative approach: Suzuki-Miyaura cross-coupling

For perform the Suzuki-Miyaura cross-coupling, the preparation of the haloarene and aryl boronic acid was required. This latter can be prepared from the haloarene compound.

The selected synthetic route for carrying out the Suzuki-Miyaura cross-coupling is presented in the Scheme 27.

This described route is composed by six steps. The first step (**S1**) corresponds to the mono-protection of diol **51**. The following step (**S2**) is the selective bromination of the mono-protected diol **57**. The third step (**S3**) consists of the alcohol silylation, necessary to perform the next step (**S4**), which is the formation of the aryl boronic acid. Then, the coupling step (**S5**) is carried out and, finally, the deprotection of the silyl ether group (**S6**) is necessary to obtain the desired product.

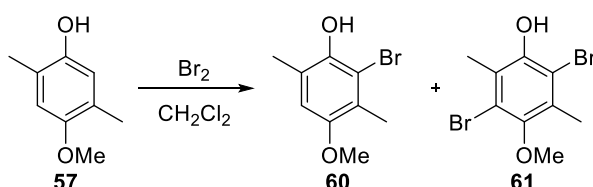


Scheme 27. Suzuki-Miyaura cross-coupling synthetic route.

4.1.2.2.1 Bromination step

The bromination of compound **57** was performed by reacting the compound **57** with Br_2 .⁴⁵ Various amounts of Br_2 were tested in order to selectively obtain the compound **60**, since the separation of the compounds **60** and **61** by flash chromatography was extremely challenging.

Table 4. Bromination of mono-protected diol **57**.



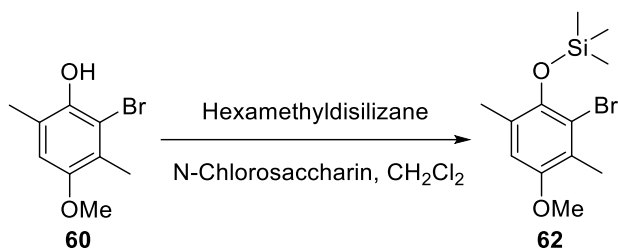
Test	Eq. Compound 7	Eq. Br_2	Results by ^1H NMR
1	1	1.1	85% of compound 60 and 15% of compound 61
2	1	1	97% of compound 60 and 3% of compound 61
3	1	0.9	97% of compound 60 and 3% of compound 57

Using the conditions of test 3, after purification by flash chromatography the reaction product **60** was isolated with high yields (92%). Since this compound was not reported in the literature, NMR characterisation was carried out to corroborate its structure.

4.1.2.2.2 Alcohol silylation step

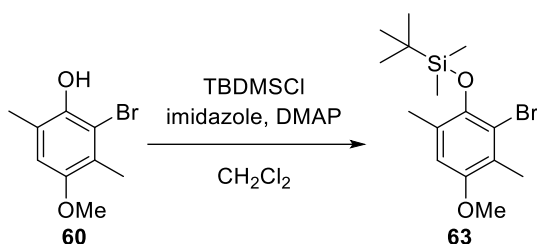
To perform the alcohol protection forming a silylether group, 2 different protecting groups were tested. We choose to form the trimethylsilyl ether and the *tert*-Butyldimethylsilyl ether because these groups readily react and are later easy to remove using a fluoride source.

- **Formation of trimethylsilyl ether:** This step was carried out by reaction of the compound **60** with hexamethyldisilazane and catalytic amounts of N-chlorosaccharin in CH_2Cl_2 .⁴⁶ After the purification the reaction product was isolated with moderate-to-high yield (78%).



Scheme 28. Alcohol protection forming a trimethylsilyl ether.

- **Formation of *tert*-Butyldimethylsilyl ether:** This step was performed reacting the compound **60** with imidazole, catalytic amounts of 4-(Dimethylamino)pyridine and *tert*-Butyldimethylsilyl chloride in CH₂Cl₂.⁴⁷ After purification by flash chromatography the product **63** was isolated in high yield (93%).



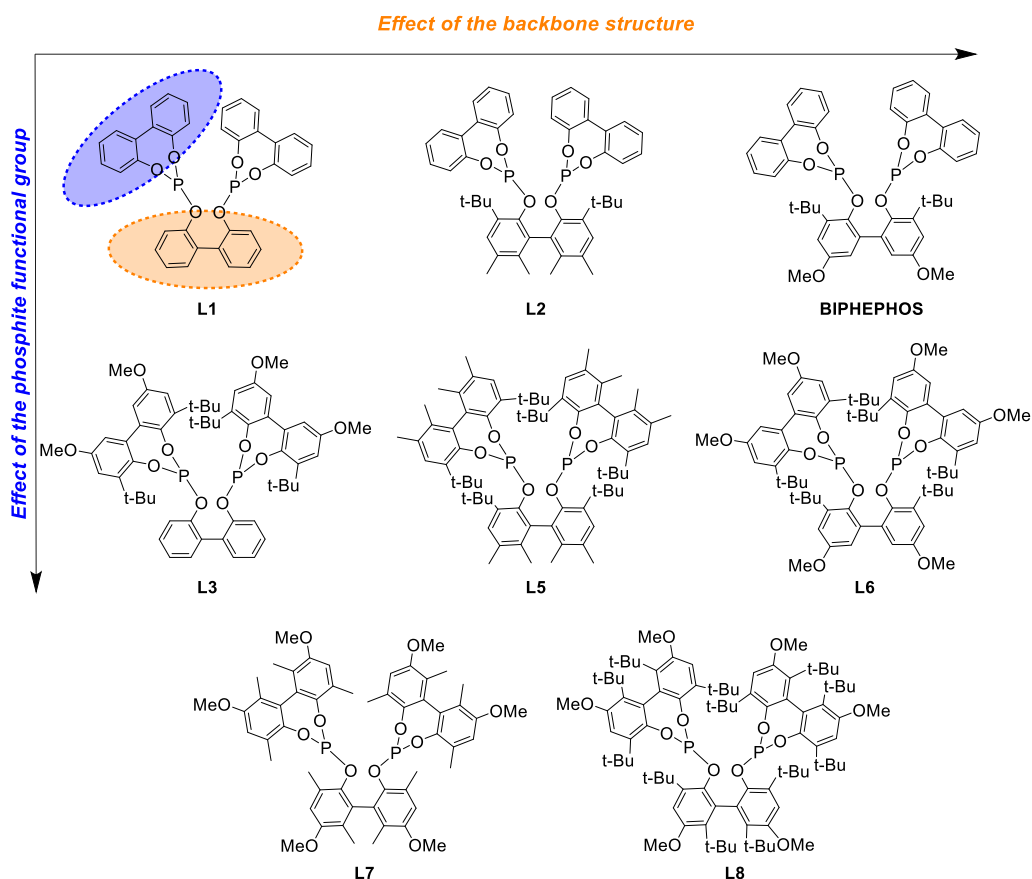
*Scheme 29. Alcohol protection forming a *tert*-Butyldimethylsilyl ether.*

The synthesis of the boronic acid reagent could not be realised due to lack of time but will be performed in the near future.

4.2. Synthesis of new diphosphite ligands

The synthesis of a family of diphosphite ligands related to BIPHEPHOS structure (Scheme 30) was carried out in order to compare the effect of the diphosphite backbone vs. the effect of the diphosphite function on the Rh-catalysed hydroformylation of styrene (activity, chemoselectivity and regioselectivity).

BIPHEPHOS ligand was selected as a suitable structure for carrying out modifications due to the interesting results provided in the Rh catalysed hydroformylation of related mono-substituted substrates.¹³

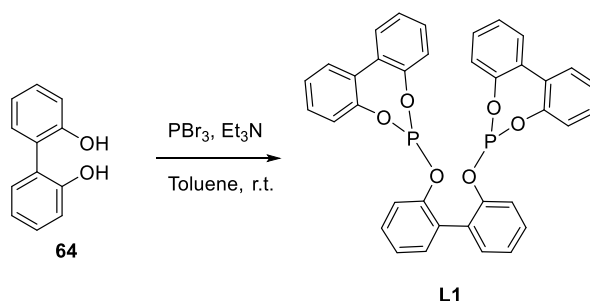


Scheme 30. Family of diphosphite ligands related to BIPHEPHOS.

4.2.1. Synthesis of diphosphite **L1**

First, we synthesise the simplest diphosphite **L1** as a reference ligand.

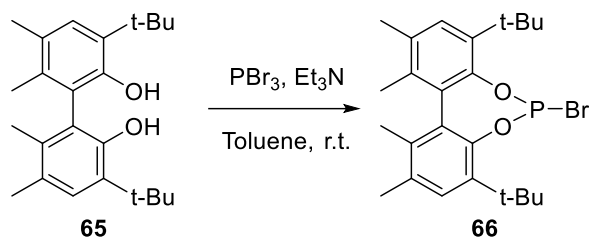
To prepare this diphosphite **L1**, a mixture of the 2,2'-biphenol (**64**), triethylamine and PBr_3 at room temperature was reacted.⁴⁸ After the purification by flash chromatography, the reaction product was isolated in low yield (13%), which was attributed to the partial decomposition of the diphosphite during the purification stages. The diphosphite **L1** was previously described in the literature and NMR characterisation details corroborated its structure.



*Scheme 31. Synthesis of diphosphite **L1**.*

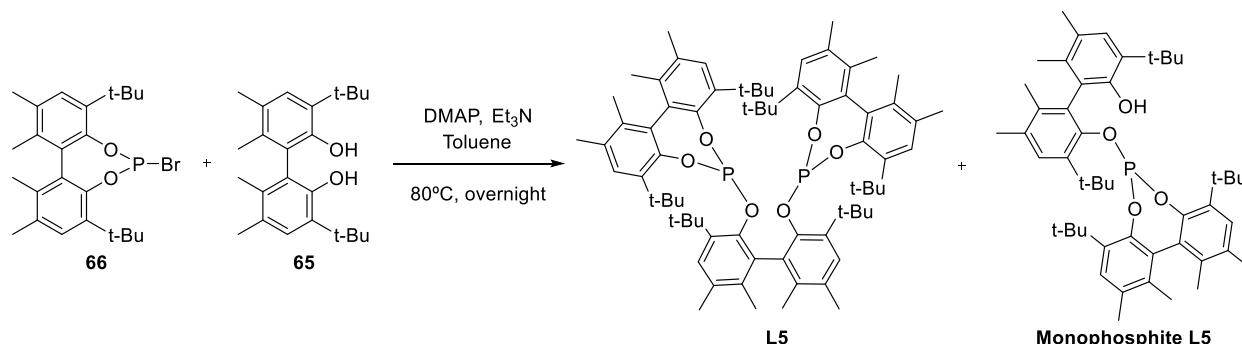
4.2.2. Synthesis of diphosphite **L5**

To synthesise the diphosphite **L5**, we first prepared the bromophosphite **66** from the biphenol **65**. To perform this step, we reacted the biphenol **65** with an excess of phosphorus tribromide and triethylamine in toluene.⁴⁹ The reaction was monitored by $^{31}\text{P}\{^1\text{H}\}$ NMR, revealing the formation of the **66** quantitatively.



*Scheme 32. Synthesis of bromophosphite **66**.*

To synthesise the diphosphite **L5**, we reacted the biphenol **65** with an excess of bromophosphite **66** (4 equiv.) in the presence of triethylamine (7 equiv.) and DMAP (0.1 equiv.) in toluene.⁴⁹

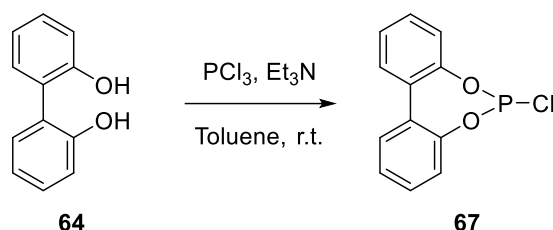


*Scheme 33. Synthesis of diphosphite **L5**.*

A solution of compound **66** and triethylamine in toluene (10 mL) was added at 0°C to a solution containing compound **65**, triethylamine and DMAP in toluene (10 mL). The reaction mixture was warmed at 80°C and stirred overnight and then filtrated. The filtrate was evaporated under reduced pressure and the residue was purified by flash chromatography. After complete characterisation by NMR and ESI-MS(+), we came to the conclusion that the product was not the ligand **L5** but probably the **Monophosphite L5**. It should be noted that the NMR was very complex because there are diastereoisomeric mixtures. To corroborate this result we also did the same reaction but with only one equivalent of compound **66** and the same product was formed, in agreement with the formation of the monophosphite. Alternative approaches to synthesise the diphosphite **L5** are currently in progress.

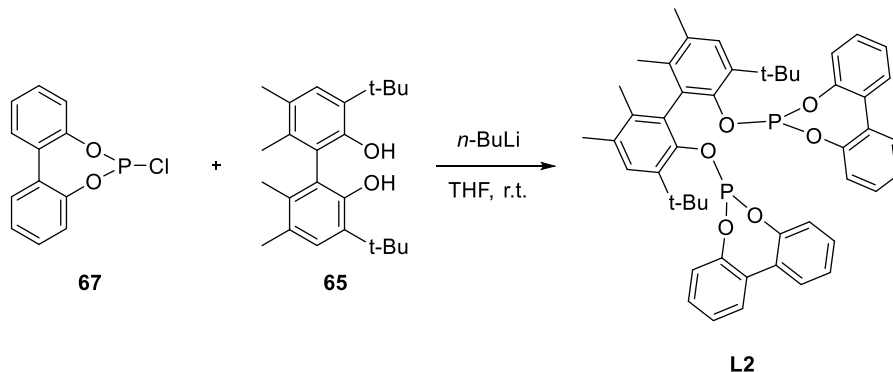
4.2.3. Synthesis of diphosphite **L2**

To synthesise the diphosphite **L2**, we first prepared the 2,2'-biphenyl chlorophosphite **67**. This step was carried out reacting the 2,2'-Biphenol (**64**) with an excess of phosphorus trichloride and triethylamine in toluene.⁵⁰ The reaction was monitored by $^{31}\text{P}\{^1\text{H}\}$ NMR, revealing the quantitative formation of **67**.



*Scheme 34. Synthesis of 2,2'-Biphenyl chlorophosphite **67**.*

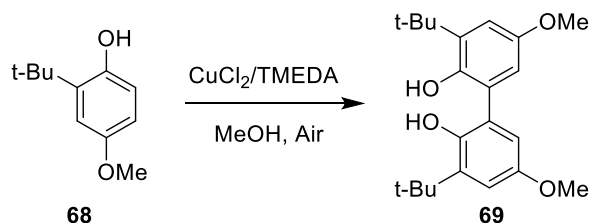
Next, we synthesise the diphosphite **L2** by reaction of the biphenol **65** with *n*-BuLi and then with an excess of chlorophosphite **67**.⁵¹ After the purification by flash chromatography the diphosphite **L2** was isolated in low yield (4%). This low yield was attributed to the partial decomposition of the diphosphite during the purification stages. The diphosphite **L2** was previously described in the literature and NMR characterisation details corroborated its structure.



*Scheme 35. Synthesis of diphosphite **L2**.*

4.2.4. Synthesis of diphosphite **L6**

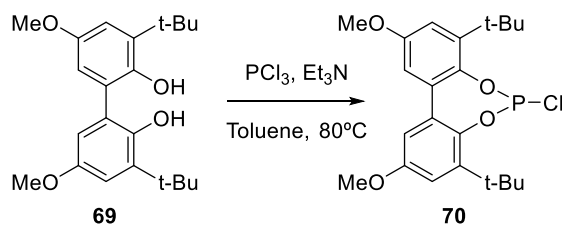
Next, we performed the synthesis of diphosphite **L6**. First, the biphenol **69** was prepared from the commercially available phenol **68**.



Scheme 36. Synthesis of biphenol 69.

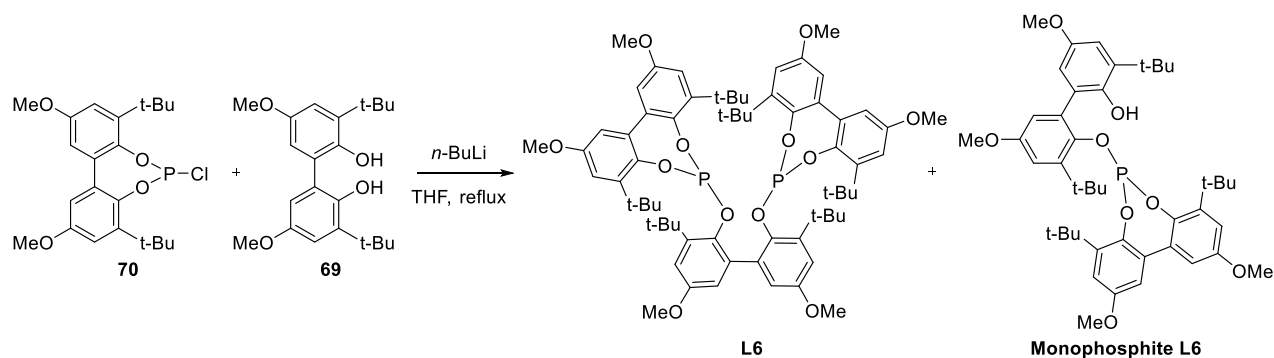
The synthesis of the biphenol **69** was carried out by reacting phenol **68** with catalytic amounts of CuCl_2 and TMEDA in MeOH under constant air flow.⁴⁴ After purification the reaction product was isolated with moderate-to-high yield (67%). The biphenol **69** was previously described in the literature and NMR characterisation details corroborated its structure.

With the biphenol **69** in hand, we performed the synthesis of the chlorophosphite **70**. This step was carried out by reaction of **69** with an excess of phosphorus trichloride and triethylamine in toluene.⁵⁰ The reaction was monitored by $^{31}\text{P}\{^1\text{H}\}$ NMR, thus revealing the quantitative formation of **70**.



Scheme 37. Synthesis of chlorophosphite 70.

At this stage, the synthesis of the diphosphite **L6** was performed by reacting the biphenol **69** in an excess of *n*-BuLi and then added to the solution of chlorophosphite **70** in THF.⁵¹



Scheme 38. Synthesis of diphosphite L6.

A solution of the biphenol **69** in THF was prepared and 3 equiv. of *n*-BuLi was added dropwise at 0°C. The reaction mixture was warmed to reflux and stirred for 2h. The reaction mixture was then cooled to 0°C, and then was added to a solution containing 3 equiv. of the chlorophosphite **70** in THF at this temperature. The mixture was then heated and stirred at reflux overnight. The mixture was quenched in water, extracted with diethyl ether and purified by flash chromatography. Similarly to the results obtained in the synthesis of **L5**, after NMR characterisation, we came to the conclusion that the product was not the ligand **L6** but the **Monophosphite L6**.

Alternative approaches to synthesise the diphosphite **L6** are currently in progress.

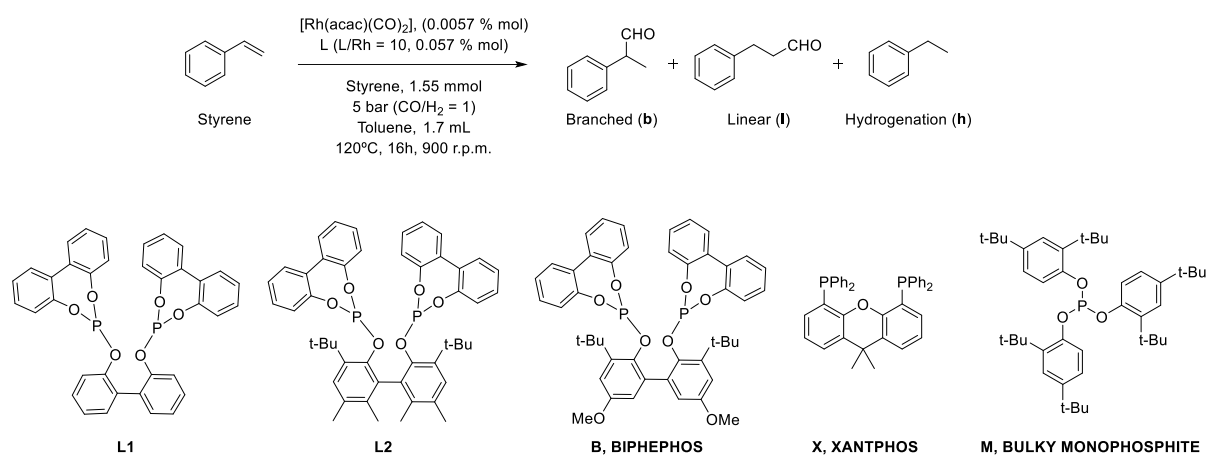
It was therefore concluded that the presence of *t*-Bu substituents in *ortho* in both the backbone and the phosphite function generates such a steric hindrance that the corresponding diphosphite ligands could not be obtained.

4.3. Rh-catalysed hydroformylation of styrene

A series of phosphite ligands was selected to perform the preliminary hydroformylation catalytic tests. The monophosphite (**M**) was selected because of the interesting results previously reported in the Rh-catalysed hydroformylation of styrene.⁵² The bidentate xantphos ligand (**X**)²⁸ and the bidentate biphephos ligand (**B**)^{13,53,54} were selected because of the excellent linear regioselectivity reported with these ligands in the Rh-catalysed hydroformylation of styrene.

The ligands prepared in this work **L1** and **L2** (structures related to biphephos) were tested under the same reaction conditions in order to evaluate the effect of the diphosphite backbone and the diphosphite function on the catalytic performance.

Table 5. Hydroformylation of styrene results



Entry ^[a]	Ligand	Conversion (%) ^[b]	Chemoselectivity (%) ^[b]	l/b ratio ^[b]	TON ^[c]
0	BLANK	0	-	-	-
1	-	5	83	1.0	877
2	X	38	98	1.0	6622
3	M	>99.9	97	1.2	17543
4	L1	4	93	1.2	764
5	L2	98	97	1.3	17193
6 ^[d]	L2	94	94	1.3	165
7	B	95	95	1.9	16636

Reaction conditions: [a] $Rh(acac)(CO)_2$ (Styrene/Rh = 17544, 0.0057 % mol), L (L/Rh = 10, 0.057 % mol), Styrene (1.55 mmol), 5 bar (CO/H₂ = 1), toluene (1.7 mL), 120°C, 16 h, 900 r.p.m.; [b] Conversion, chemoselectivity and regioselectivity determined by ¹H NMR; [c] TON defined as the mole of styrene converted, divided by the moles of Rh; [d] $Rh(acac)(CO)_2$ (Styrene/Rh = 175, 0.057 % mol).

Catalytic test with the Rh-unmodified species provided very low conversions with moderate chemoselectivities and a regioselectivity to the linear aldehyde of 1.0 (entry 1, Table 5).

Under our reaction conditions, the use of xantphos provided low-to-moderate conversions, and a better chemoselectivity and same regioselectivity than the unmodified Rh-catalyst (entry 1 vs. entry 2, Table 5). The bulky mono-phosphite ligand **M** (entry 3 vs. entry 2, Table 5) produced quantitative conversions with improved chemo- and regioselectivity to the linear product than the xantphos ligand.

Diphosphite ligands (entry 4, 5, 6 and 7, Table 5) provided moderate-to-high conversions with similar chemoselectivities and higher regioselectivities to the linear product than the bulky monophosphite **M** (entry 3, Table 5).

Among the diphosphite ligands, ligand **L2** and **B** produced much higher conversions and similar chemoselectivities than ligand **L1** (entry 5, 6, 7 vs. entry 4, Table 5). Then, it seems that the presence of electron-donating and bulky substituents in the backbone structure (*tert*-

butyl, methyl and methoxy) contributed to the enhancement of the catalytic activity and without effect in the chemio-selectivity. The highest regioselectivity was achieved with the ligand **B** (entry 7, Table 5) that contains a methoxy groups in *para* positions of the backbone.

In conclusion, our study revealed that the diphosphite ligands with electron-donating (*para* methoxy) and bulky (*ortho* tert-butyl) substituents in the backbone structure are the most appropriated for obtaining high activities and regioselectivities to the styrene derived linear aldehyde.

5. Conclusions.

We have successfully completed the main objective of this work which was to explore the hydrocinnamaldehyde production by Rh-diphosphite reverse regioselective hydroformylation of styrene.

Concerning the partial objectives:

1. Novel synthetic routes for the synthesis of new atropisomeric backbones have been designed and partially completed with success. The last step of the synthesis (coupling of the phenol units) is currently in progress and the products obtained from this reaction will be directly applied in the synthesis of new diphosphite ligands.
2. Experimental procedures were developed for the production of phosphorochloridites, phosphorobromidites and diphosphites. Due to the high tendency to be hydrolysed under the acidic conditions used during the purification stage, moderate-to-low yields were sometimes obtained. Optimization of the reaction conditions and purification procedures are in progress.
3. Evaluation of the synthesised and commercial ligands in the Rh-catalysed hydroformylation of styrene was successfully completed. With the catalytic results revealed that the diphosphite ligands with electron-donating (*para* methoxy) and bulky (*ortho* tert-butyl) substituents in the backbone structure are the most appropriate for obtaining high activities and regioselectivities to the styrene derived linear aldehyde. The study of the effect of the phosphite function on the catalytic performance is in progress. The highest regioselectivity was obtained is with the BIPHEPHOS ligand and we are currently evaluating structural modifications of this ligand.

6. Experimental part

Solvents and reagents were obtained from commercial sources (Sigma-Aldrich and Alfa-Aesar) and were purified and dried according to standard procedures.⁵⁵ Air sensitive reactions were performed using standard Schlenk techniques under argon in dry solvents. Flash column chromatography was carried out using a forced flow of the indicated solvent on Merck silica gel 60 (230–400 mesh). Reactions were monitored by TLC carried out on 0.25 mm E. Merck silica gel 60 F₂₅₄ aluminium plates.

1D (¹H, ¹³C{¹H} and ³¹P{¹H}) and 2D (¹H-¹H COSY, ¹H-¹³C HSQC and ¹H-¹³C HMBC) NMR spectra were recorded on a Varian Mercury 400 MHz spectrometer. Chemical shifts (δ) are reported in parts per million (ppm) and referenced to residual solvent or tetramethylsilane. Mass Spectra were recorded on a Waters LCT Premier Spectrometer (ESI).

2,5-dimethylhydroquinone(52).³⁴ Compound **52** was prepared from commercially available 2,5-dimethyl-1,4-benzoquinone (compound **51**). To a vigorously stirred mixture of compound **51** (2.5 g, 18.4 mmol, 1equiv.) in ether (50 mL), MeOH (25 mL) and water (100 mL), NaBH₄ was added (3.5 g, 91.9 mmol, 5 equiv.). After 15 min the mixture was acidified with a HCl solution (1M), then the mixture was extracted with ether (3 x 50 mL). The combined ether layers were washed with brine, dried over MgSO₄, and evaporated to give compound **52** in 93% yield (2354.7 mg, 17.1 mmol) as a white solid. ¹H NMR (400MHz, DMSO-*d*₆) δ 8.30 (s, 2H), 6.44 (s, 2H), 1.99 (s, 6H).

1,4-dimethoxy-2,5-dimethylbenzene (54).³⁷ Under argon atmosphere, to a solution of compound **52** (1000 mg, 7.24 mmol, 1 equiv.) in dry THF (72.4 mL) NaH (889.6 mg, 60%, 22.24 mmol, 3.07 equiv.) was added at 0°C and the solution was stirred at the same temperature for 15 min. MeI (11.01 mL, 72.4 mmol, 10 equiv.) was added to the reaction mixture at 0°C, the resulting solution was stirred at the same temperature 15 min and then at room temperature for 24 h. In the reaction mixture saturated NH₄Cl_{aq} (36.2 mL) was added, then THF was removed by rotatory evaporator. The aqueous solution was extracted with EtOAc (10 mL x 3). The organic phases were combined, washed with brine, dried over MgSO₄ and evaporated. The residue was purified by flash chromatography (silica gel/hexane-EtOAc, 9:1 v/v) to give compound **54** in 68% yield (822.4 mg, 4.95 mmol) as a white solid. ¹H NMR (400MHz, CDCl₃) δ 6.66 (s, 2H), 3.78 (s, 6H), 2.21 (s, 6H); ¹³C{¹H} NMR (100 MHz, CDCl₃) δ 151.47 (2C), 124.29 (2C), 113.77 (2C), 56.14 (2C), 16.04 (2C).

4-methoxy-2,5-dimethylphenol (57).⁴² Under argon atmosphere, compound **52** (1317.8 mg, 9.54 mmol, 1 equiv.), H₂SO₄ (935.67 mg, 9.54 mmol, 1 equiv.) and NaNO₂ (33.12 mg, 0.48 mmol, 0.05 equiv.) were stirred in methanol (19.1 mL) at room temperature for 12 h. The mixture was quenched in water (40 mL) and extracted with CH₂Cl₂ (40 mL x 3). The organic phases were combined, dried over MgSO₄ and evaporated. The residue was purified by flash chromatography (silica gel/ hexane-EtOAc, 99:1 v/v) to give compound **57** in 92% yield (1330.3 mg, 8.75 mmol) as a white solid. ¹H NMR (400MHz, CDCl₃) δ 6.60 (s, 1H), 6.59 (s, 1H), 4.23 (s, 1H), 3.77 (s, 3H), 2.22 (s, 3H), 2.15 (s, 3H); ¹³C{¹H} NMR (100 MHz, CDCl₃) δ 151.89, 147.30, 125.31, 121.24, 117.79, 113.61, 56.28, 15.88, 15.83.

2-bromo-4-methoxy-3,6-dimethylphenol (60).⁴⁵ A solution of compound **57** (127.0 mg, 0.835 mmol, 1.0 equiv.) in CH₂Cl₂ (5.45 mL) with continuous stirring was cooled to 0°C followed by slow addition of bromine (120.11 mg, 0.752 mmol, 0.9 equiv.). After addition, the cooling bath was removed and the mixture was stirred at room temperature for another 90 min. The reaction was quenched by addition of saturated aqueous solution Na₂S₂O₃ (3mL) and H₂O (2mL). The phases were separated and the aqueous layer was extracted with CH₂Cl₂ (3x10 mL). The organic phases were combined, dried over MgSO₄ and evaporated. The residue was purified by flash chromatography (silica gel/ hexane-EtOAc, 99:1 v/v) to give compound **60** in 92% yield (177.4 mg, 0.77 mmol) as a white solid. ¹H NMR (400MHz, CDCl₃) δ 6.63 (s, 1H), 5.30 (s, 1H), 3.77 (s, 3H), 2.28 (s, 6H); ¹³C{¹H} NMR (100 MHz, CDCl₃) δ 151.29, 144.48, 124.26, 122.04, 114.31, 113.11, 56.67, 17.00, 16.10.

(2-bromo-4-methoxy-3,6-dimethylphenoxy)trimethylsilane (62).⁴⁶ In a flask containing the compound **60** (0.43 mmol, 100 mg, 1 equiv.), hexamethyldisilazane (0.52 mmol, 83.3 mg, 1.2 equiv.) and CH₂Cl₂ (0.3 mL) the *N*-chlorosaccharin was added (4.3·10⁻³ mmol, 0.94 mg, 0.01 equiv.). The reaction mixture was stirred at room temperature overnight. The CH₂Cl₂ was evaporated under reduced pressure and *n*-hexane (3 mL) was added to the reaction mixture. The resulting mixture was filtered and the residue was washed with *n*-hexane. Evaporation of *n*-hexane gives the compound **62** in 78% yield (101.7 mg, 0.34 mmol) as an orange oil. ¹H NMR (400 MHz, CDCl₃) δ 6.59 (s, 1H), 3.77 (s, 3H), 2.29 (s, 3H), 2.24 (s, 3H), 0.30 (s, 9H); ¹³C{¹H} NMR (100 MHz, CDCl₃) δ 152.19, 145.26, 126.75, 125.18, 119.69, 111.94, 56.26, 18.57, 16.41, 1.23 (3 C).

(2-bromo-4-methoxy-3,6-dimethylphenoxy)(tert-butyl)dimethylsilane (63).⁴⁷ The compound **60** (200 mg, 0.87 mmol, 1 equiv.), TBDMSCl (196.7 mg, 1.305 mmol, 1.5 equiv.), imidazole (236.92 mg, 3.48 mmol, 4 equiv.) and DMAP (10.6 mg, 0.087 mmol, 0.1 equiv.)

were stirred in CH₂Cl₂ (1.4 mL) at room temperature overnight. The reaction was quenched by addition of aqueous HCl 1.0 M (3 mL). The phases were separated and the aqueous phase was extracted with CH₂Cl₂ (3x3 mL). The organic phases were combined, dried over MgSO₄ and evaporated. The residue was purified by flash chromatography (silica gel/ 100% CH₂Cl₂) to give the compound **63** in 93 % yield (280.0 mg, 0.81 mmol) as a colourless oil. ¹H NMR (400MHz, CDCl₃) δ 6.58 (s,1H), 3.77 (s, 3H), 2.28 (s, 3H), 2.24 (s, 3H), 1.04 (s, 9H), 0.24 (s, 6H); ¹³C{¹H} NMR (100 MHz, CDCl₃) δ 152.11, 144.82, 126.70, 125.43, 119.65, 112.19, 56.29, 26.40 (3C), 19.01, 18.68, 16.47, -2.36 (2C).

Diphosphite L1.⁴⁸ A solution of 2,2'-biphenol (1000 mg, 5.4 mmol, 1 equiv.) in toluene (15 mL) was added triethylamine (3817.8 mg, 37.8 mmol, 7 equiv.). The solution was cooled at 0°C and slowly added PBr₃ (1593 mg, 5.9 mmol, 1.1 equiv.). The reaction mixture was warm at room temperature and stirred 16h and then filtrated. The filtrated was evaporated under reduced pressure. The residue was purified by flash chromatography (silica gel/ hexane-DCM, 7:3 v/v) to give the diphosphite **L1** in 13% yield (139.1 mg, 0.23 mmol) as a white solid. ¹H NMR (400MHz, CDCl₃) δ 7.40 (m, 8H), 7.32 (m, 2H), 7.22 (m, 10H), 6.88 (m, 4H); ³¹P{¹H} NMR (161.9MHz, CDCl₃): δ 144.43 (s).

Bromophosphite 66.⁴⁹ A solution of compound **65** (1000 mg, 2.82 mmol, 1 equiv.) in toluene (20 mL) was added triethylamine (1993.7 mg, 19.74 mmol, 7 equiv.). The solution was cooled at 0°C and slowly added PBr₃ (839.7 mg, 3.11 mmol, 1.1 equiv.). The reaction mixture was warm at room temperature and stirred for 18h and then filtrated. The filtrate was evaporated under reduced pressure to give the bromophosphite **66** in quantitative yield (determinate by ³¹P{¹H} NMR) (1306.79 mg, 2.82 mmol) as a yellow oil. ³¹P{¹H} NMR (161.9MHz, toluene-*d*₈): δ 181.23 (s).

2,2'-Biphenyl chlorophosphite (67).⁵⁰ 2,2'-Biphenol (**64**) (1000 mg, 5.37 mmol, 1 equiv.) was dissolved in toluene (17.5 mL) and the solution was cooled to 0°C. A solution of phosphorous trichloride (1112.4 mg, 8.1 mmol, 1.5 equiv.) and triethylamine (1627.1 mg, 16.1 mmol, 3 equiv.) in toluene (10 mL) was slowly added. The mixture was warmed to room temperature and stirred for 36 hours. It was filtered and the solvent evaporated under reduce pressure to give the chlorophosphite **67** in quantitative yield (determinate by ³¹P{¹H} NMR) (1342.5 mg, 5.37 mmol) as a yellow oil. ³¹P{¹H} NMR (161.9MHz, toluene-*d*₈): δ 179.43 (s).

Diphosphite L2.⁵¹ To a solution of the biphenol **65** (592.06 mg, 1.67 mmol, 1 equiv.) in THF (20 mL) at 0°C was added dropwise *n*-BuLi (5.0 mmol, 3.13 mL of 1.6 M hexane solution).

The reaction mixture was warmed to room temperature and stirred for 2h at reflux. The reaction mixture was then cooled to 0°C, and then was added to a solution of the chlorophosphite **67** (1253 mg, 5.0 mmol, 3 equiv.) in THF (10 mL) at 0°C. After the addition the cooling bath was removed and the mixture was stirred at room temperature overnight. The mixture was quenched in water (20 mL) and extracted with diethyl ether (30 mL x 3). The organic phases were combined, dried over MgSO₄ and evaporated. The residue was purified by flash chromatography (silica gel/ 100% hexane) to give the diphosphite **L2** in 4% yield (50.8 mg, 0.065 mmol) as a yellow oil. ¹H NMR (400MHz, CDCl₃) δ 7.33 (m, 4H), 7.18 (m, 6H), 7.03 (m, 6H), 6.88 (m, 2H), 2.25 (s, 6H), 1.83 (s, 6H), 1.28 (s, 18H); ³¹P{¹H} NMR (161.9MHz, CDCl₃) δ 142.46 (s).

Biphenol 69.⁴⁴ In a three-necked round bottomed flask equipped with a gas inlet the phenol **68** (20 g, 0.11 mol, 1 equiv.) was dissolved in methanol (40 mL), anhydrous CuCl₂ (92.43 mg, 6.875·10⁻⁴mol, 6.25·10⁻³ equiv.) and N,N,N',N'-Tetramethylethylenediamine (0.12 g, 1.033·10⁻³mol, 9.375·10⁻³ equiv.) were added. The reaction mixture was stirred for 24h under a continuous flow of air. After 24h the precipitate was filtered and washed with cold methanol and dried in vacuum. The compound **69** was obtained in 67% yield (13.38 g, 37.31 mmol) as a white solid. ¹H NMR (400MHz, CDCl₃) δ 6.96 (d, *J* = 3.1 Hz, 2H), 6.62 (d, *J* = 3.1 Hz, 2H), 5.02 (s, 2H), 3.78 (s, 6H), 1.43 (s, 18H).

Chlorophosphite 70.⁵⁰ A solution of PCl₃ (407.87 mg, 2.97 mmol, 1.35 equiv.) and triethylamine (1565.5 mg, 15.5 mmol, 7 equiv.) was cooled to 0°C. A solution of Biphenol **69** (788.66 mg, 2.2 mmol, 1 equiv.), triethylamine (1565.5 mg, 15.5 mmol, 7 equiv.) dissolved in toluene (27 mL) was slowly added. The mixture was warmed to 80°C and stirred for 12 hours. The reaction mixture was filtered and the solvent evaporated under reduce pressure to give the chlorophosphite **70** in quantitative yield (determinate by ³¹P{¹H} NMR) (930.36 mg, 2.2 mmol) as a yellow oil. ³¹P{¹H} NMR (161.9MHz, toluene-*d*₆): δ 172.80 (s)

- Equipment for hydroformylation process:

HEL7: Seven tubes reactor (7 x 10 mL), equipped with seven glass inner beakers, and a magnetic stirring.

HEL1: Single component 25 mL reactor, equipped with one Teflon tube, and a magnetic stirring



Figure 2. Reactor HEL7 in the left and reactor HEL1 in the right.

7. References

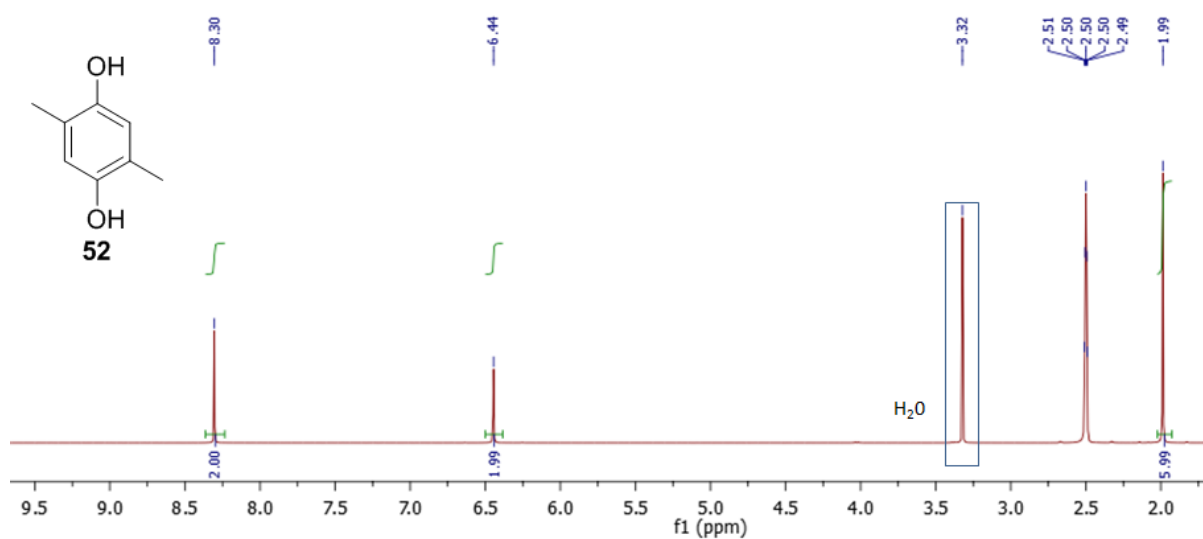
- (1) Roelen, O.; *Chem. Abstr.* **1994**, 38, 550
- (2) Cornils, B.; Hermann, W.A. (ed.) *Applied Homogeneous Catalysis with Organometallic Compounds*, vol. 1, Wiley-VCH, Weinheim, **2002**
- (3) a) Klosin, J.; Landis, C.R. *Acc. Chem. Res.* **2007**, 40, 1251-1259; b) Gual, A.; Godard, C.; Castellón, S.; Claver, C. *Tetrahedron: Asymmetry*, **2010**, 21, 1135-1146; c) van Leeuwen, P. W. N. M.; Kamer, P. C. J.; Claver, C.; Pàmies, O.; Diéguez, M. *Chem. Rev.* **2011**, 111, 2077-2118
- (4) Breit, B. in *Aldehydes: synthesis by hydroformylation of alkenes in Science of synthesis*, Brückner, R., vol. 25, Thieme, Stuttgart, **2007**.
- (5) van Leeuwen, P.W.N.M. in *Homogeneous Catalysis: Understanding the Art*, Kluwer, Dordrecht, **2004** and references therein
- (6) Breit, B. *Acc. Chem. Res.* **2003**, 36, 264-275
- (7) Eilbracht, P.; Schmidt, A.M. *Top. Organomet. Chem.* **2006**, 18, 65-95
- (8) Evans, D.A.; Osborn, J.A.; Wilkinson, G.; *J. Chem. Soc. A* **1968**, 3133-3142
- (9) van Leeuwen, P.W.N.M.; Claver, C. in *Rhodium catalysed hydroformylation*, Kluwer, Dordrecht, **2000** and references therein
- (10) Jongsma, T.; Challa, G.; van Leeuwen, P.W.N.M. *J. Organomet. Chem.* **1991**, 421, 121-128
- (11) Siegbahn, P. E. M. *J. Am. Chem. Soc.* **1993**, 115, 5803-5812
- (12) Keulemans, A.I.M.; Kwantes, A.; van Bavel, T. *Rec. Trav. Chim. Pays Bas.* **1948**, 67, 298-308.
- (13) Gusevskaya, E. V.; Jiménez-Pinto, J.; Börner, A. *ChemCatChem*, **2014**, 6, 382-411
- (14) *The Chemistry of Fragrances*, 2nd ed. (Ed.: C. Sell), Royal Society of Chemistry, Cambridge, **2006**, p. 53.
- (15) http://www.leffingwell.com/top_10.htm. (Date of query: 10/05/2018)
- (16) V. Rautenstrauch, M. Lindstrøm, B. Bourdin, J. Currie, E. Oliveros, *Helv. Chim. Acta.* **1993**, 76, 607-615.
- (17) Heck, R.F. *Acc. Chem. Res.* **1969**, 2, 10-16.
- (18) Kamer, P.C. J.; van Rooy, A.; Schoemaker, G.C.; van Leeuwen, P.W.N.M. *Coord. Chem. Rev.* **2004**, 248, 2409-2424.
- (19) van der Veen, L. A.; Boele, M. D. K.; Bregman, F. R.; Kamer, P. C. J.; van Leeuwen, P. W. N. M.; Kees, G.; Fraanje, J.; Schenck, H.; Bo, C. *J. Am. Chem. Soc.* **1998**, 120, 11616-11626
- (20) van der Veen, L. A.; Keeven, P. H.; Schoemaker, G. C.; Reek, J. N. H.; Kamer, P. C. J.; van Leeuwen, P. W. N. M.; Lutz, M.; Spek, A. L. *Organometallics*. **2000**, 19, 872-883;
- (21) Deutsch, P.P.; Eisenberg, R. *Organometallics*. **1990**, 9, 709-718.
- (22) Dieguez, M.; Pamies, O.; Ruiz, A.; Castillon, S.; Claver, C. *Chem.Eur. J.* **2001**, 7, 3086-3094
- (23) R. Lazzaroni, A. Raffaelli, R. Settambolo, S. Bertozzi and G. Vitulli, *J. Mol. Catal.*, **1989**, 50, 1.

- (24) Brown, J. M.; Kent, A. G. J. *Chem. Soc., Perkin Trans. 2*, **1987**, 1597-1607
- (25) Van der Veen, L.A.; Keeven, P. H.; Schoenmaker, G. C.; Reek, J. N. H.; Kamer, P. C. J.; Van Leeuwen, P. W. N. M.; Lutz, M.; Spek, A. L. *Organometallics*. **2000**, 872-883.
- (26) Kramer, P. C. J.; van Leeuwen, P. W. N. M.; Reek J. N. H. *Acc. Chem. Res.* **2001**, 34, 895-904.
- (27) Van der Veen, L.A.; Boele, M. D. K.; Bregman, F. R.; Kamer, P. C. J.; van Leeuwen, P. W. N. M.; Goubitz, K.; Fraanje, J. Shenk, H.; Bo, C. *J. Am. Chem. Soc.* **1998**, 120, 11616-11626.
- (28) Kranenburg, M.; van der Burgt, Y. E. M.; Kamer, P. C. J.; van Leeuwen, P. W. N. M., *Organometallics*, **1995**, 14, 3081-3089.
- (29) Semeril, D.; Matt, D.; Toupet, L.; Oberhauser, W.; Bianchini, C., *Chem. Eur. J.* **2010**, 16, 13843-13849.
- (30) Yu, S.; Chie, Y.; Guan, Z.; Zou, Y.; Li, W.; Zhang, X. *Org Lett.* **2009**, 241-244.
- (31) P. C. J. Kamer and P. W. N. M. van Leeuwen, *Phosphorus(III) Ligands in Homogeneous Catalysis: Design and Synthesis*, John Wiley and Sons, Chichester, **2012**
- (32) Boymans, E.; Janssen, M.; Müller, C.; Lutz, M.; Vogt, D. *Dalton Trans.* **2013**, 137-142.
- (33) Zheng, C; Mo M.; Liang H.; Zheng X.; Fu H.; Yuan M.; Li R.; Chen H.; *Appl. Organomet. Chem.* **2013**, 27, 474-478.
- (34) Walton, D. P.; Dougherty, D. A. *J. Am. Chem. Soc.* **2017**, 139 (13), 4655–4658.
- (35) Libman, A.; Shalit, H.; Vainer, Y.; Narute, S.; Kozuch, S.; Pappo, D. *J. Am. Chem. Soc.* **2015**, 137, 11453–11460.
- (36) Jiang, C.; Garg, S.; Waite, T. D. *Environ. Sci. Technol.* **2015**, 49 (24), 14076–14084.
- (37) Kamimura, A.; Nokubi, T.; Watanabe, R.; Ishikawa, M.; Nasu, K.; Uno, H.; Sumimoto, M. *J. Org. Chem.* **2014**, 79 (3), 1068–1083.
- (38) Liao, B. B.; Milgram, B. C.; Shair, M. D. *J. Am. Chem. Soc.* **2012**, 134 (40), 16765–16772.
- (39) Love, B. E.; Bonner-Stewart, J.; Forrest, L. A. *Synlett.* **2009**, No. 5, 813–817.
- (40) Chattopadhyay, B.; Ghosh, S.; Mondal, S.; Mukherjee, M.; Mukherjee, A. K. *CrystEngComm.* **2012**, 14 (3), 837–846.
- (41) Takizawa, Yasuomi; Hitomi, Masakatsu; Miyachi, Hiroyuki; Yoshihara, Nobutoshi; Takizawa, Junko; Yamamoto, H. *J. Jpn. Oil Chem. Soc.* **1995**, 44 (9), 669–670.
- (42) Gambarotti, C.; Melone, L.; Punta, C.; Shisodia, S. U. *Curr. Org. Chem.* **2013**, 17, 1108–1113.
- (43) Chen, J.; Liu, D.; Fan, D.; Liu, Y.; Zhang, W. *Tetrahedron.* **2013**, 69 (38), 8161–8168.
- (44) Buisman, G. J. H.; Kamer, P. C. J.; van Leeuwen, P. W. N. M. *Tetrahedron: Asymmetry.* **1993**, 4 (7), 1625–1634.
- (45) Tietze, L. F.; Hungerland, T.; Düfert, A.; Objartel, I.; Stalke, D. *Chem. Eur. J.* **2012**, 18, 3286–3291.
- (46) Aghapour, G.; Moghaddam, A. K.; Nadali, S. *J. Chin. Chem. Soc.* **2015**, 62, 197–203.
- (47) Pereira, A. R.; Strangman, W. K.; Marion, F.; Feldberg, L.; Roll, D.; Mallon, R.; Hollander, I.; Andersen, R. *J. Med. Chem.* **2010**, 53, 8523–8533.

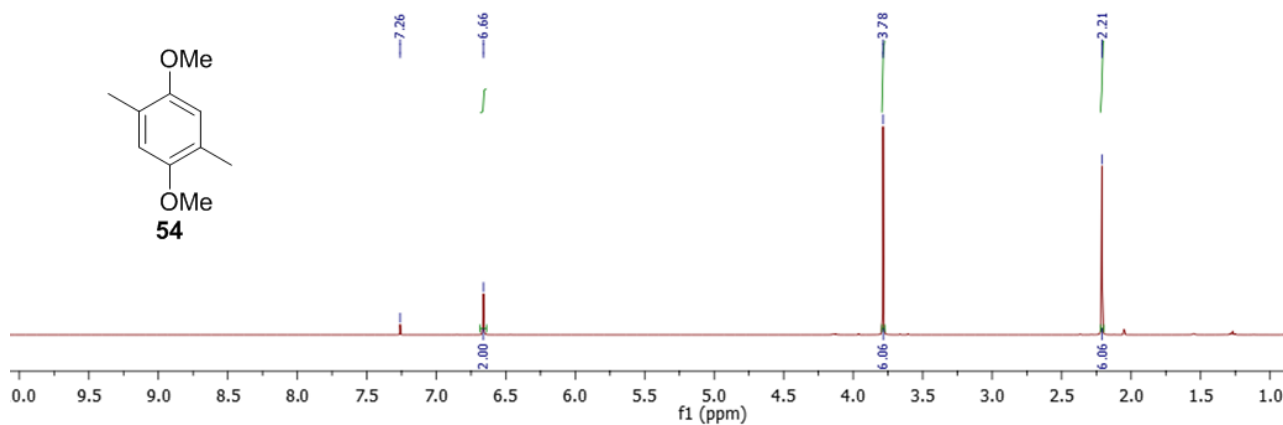
- (48) Meyer, T. G.; Fischer, A.; Jones, P. G.; Schmutzler, R. *Z. Naturforsch.* **1993**, 48 b, 659-671
- (49) Cobley, C. J.; Froese, R. D. J.; Klosin, J.; Qin, C.; Whiteker, G. T.; Abboud, K. A. *Organometallics.* **2007**, 26, 2986–2999.
- (50) Vallée, C.; Chauvin, Y.; Basset, J.-M.; Santini, C. C.; Galland, J. C. *Adv. Synth. Catal.* **2005**, 347, 1835–1847.
- (51) Zou, Y.; Yan, Y.; Zhang, X. *Tetrahedron Lett.* **2007**, 48, 4781–4784.
- (52) van Rooy, A.; Orij, E. N.; Kamer, P. C. J.; van Leeuwen, P. W. N. M. *Organometallics.* **1995**, 14, 34-43
- (53) Billig, E.; Abatjoglou, A. G.; Bryant, D. R. U.S. Pat. 4,668,651; Eur. Pat. Appl. 213,639, 1987 (to Union Carbide); *Chem. Abstr.* **1987**, 107, 7392
- (54) Billig, E.; Abatjoglou, A. G.; Bryant, D. R.; Murray, R. E.; Maher, J. M. U.S. Pat. 4,599,206, 1986 (to Union carbide); *Chem. Abstr.* **1988**, 109, 233177
- (55) D. D. Perrin, W. L. F. Armarego and D. R. Perrin, *Purification of laboratory chemicals*, Pergamon Press, Oxford, New York, **1980**

8. Supporting information: NMR spectra of products and intermediates

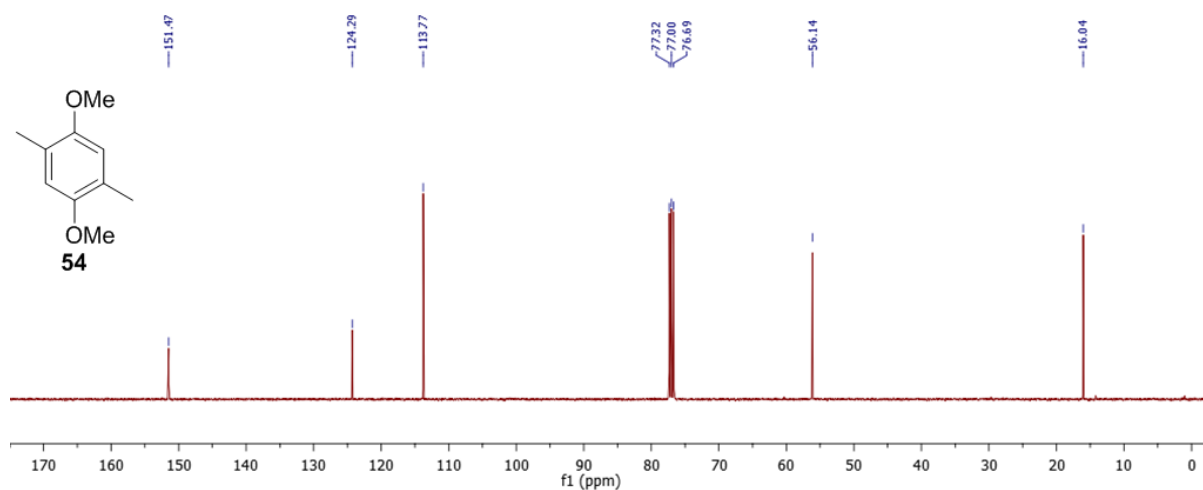
^1H spectrum of **52** ($\text{DMSO-}d_6$, RT)



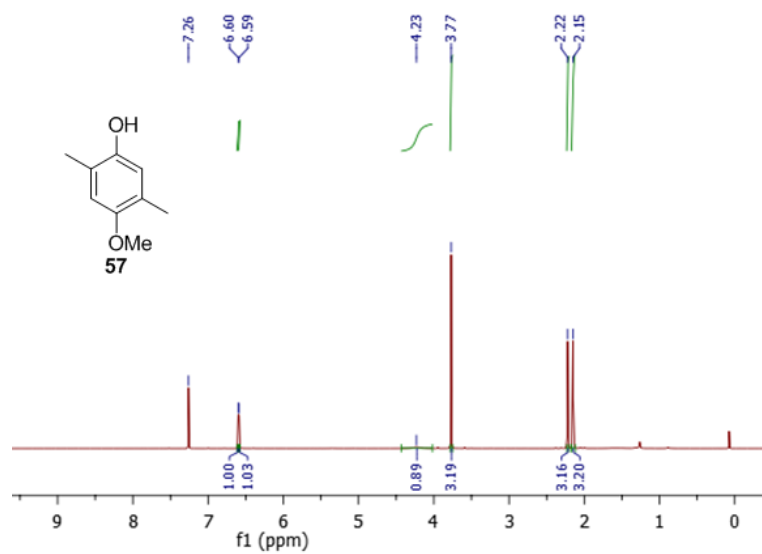
^1H spectrum of **54** (CDCl_3 , RT)



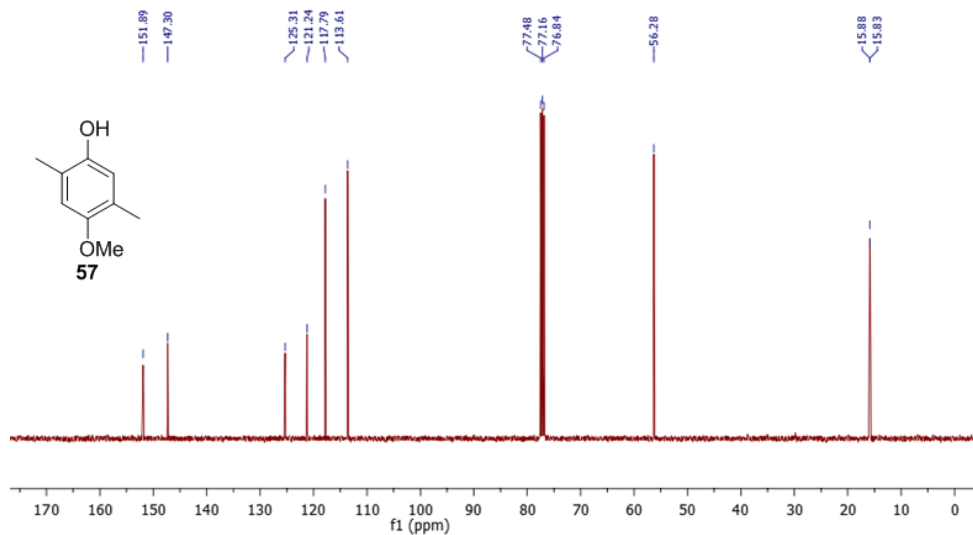
$^{13}\text{C}\{^1\text{H}\}$ spectrum of **54** (CDCl_3 , RT)



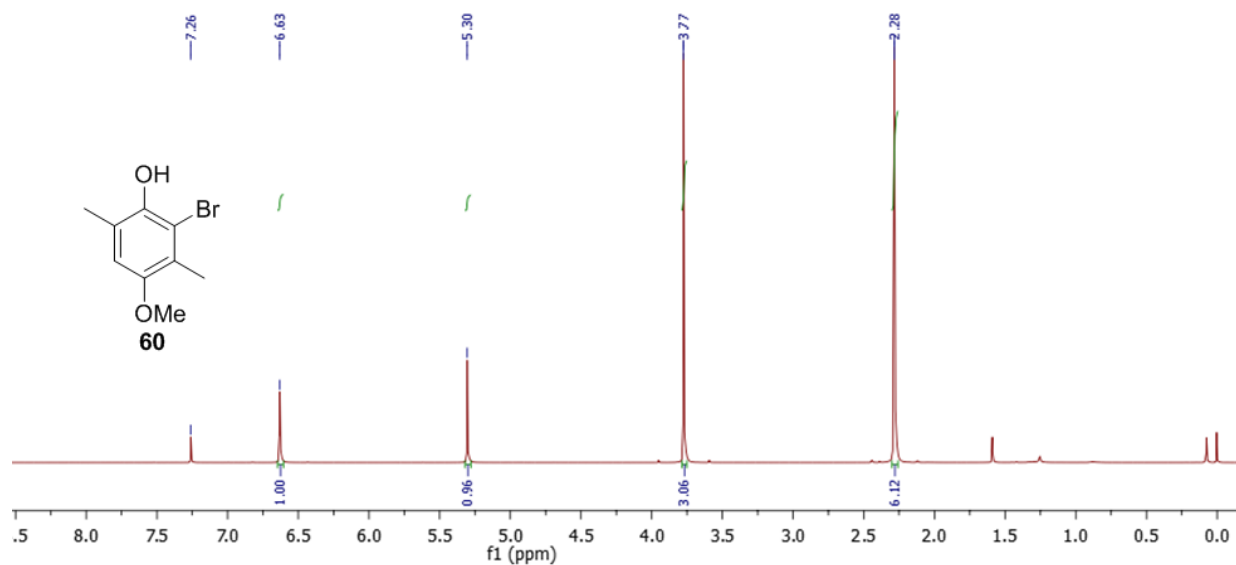
^1H spectrum of **57** (CDCl_3 , RT)



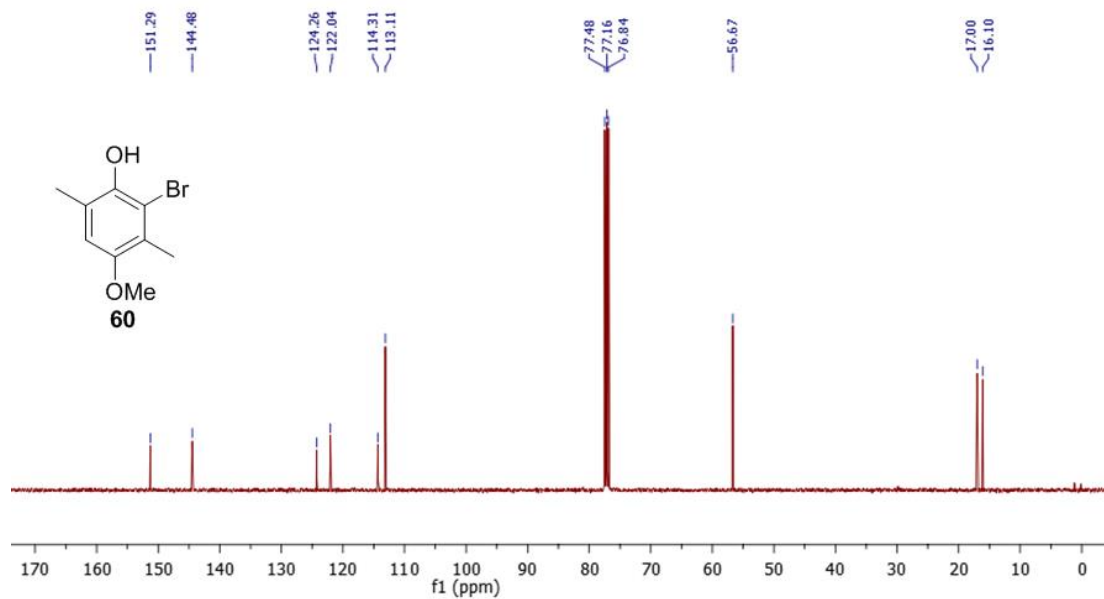
$^{13}\text{C}\{^1\text{H}\}$ spectrum of **57** (CDCl_3 , RT)



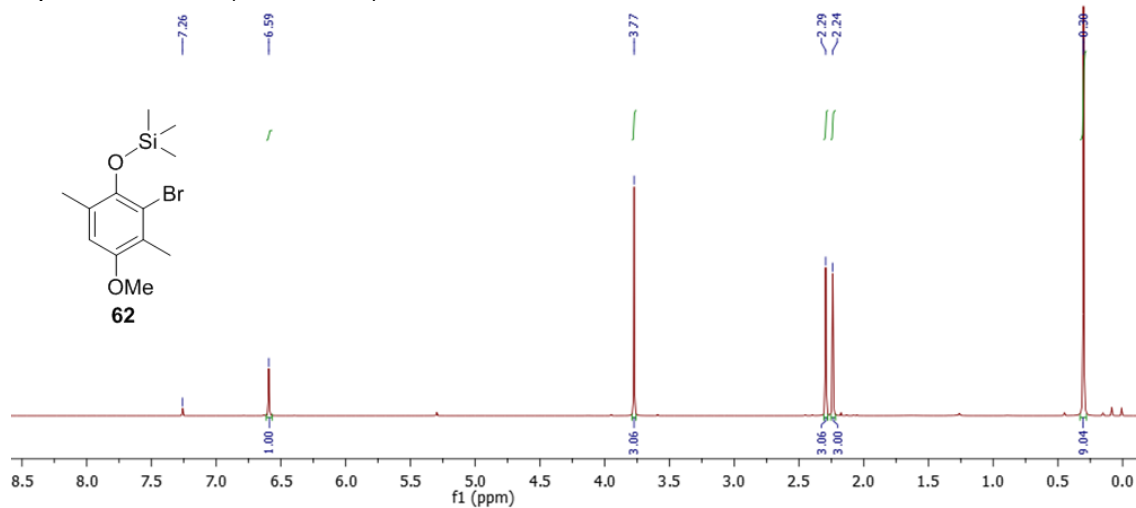
^1H spectrum of **60** (CDCl_3 , RT)



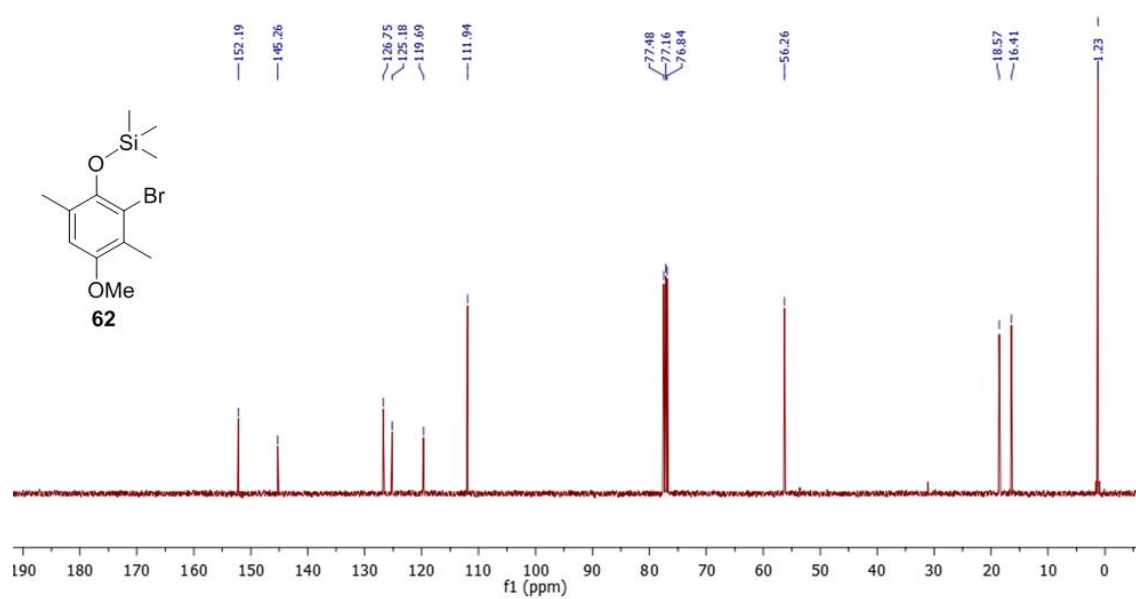
$^{13}\text{C}\{^1\text{H}\}$ spectrum of **60** (CDCl_3 , RT)



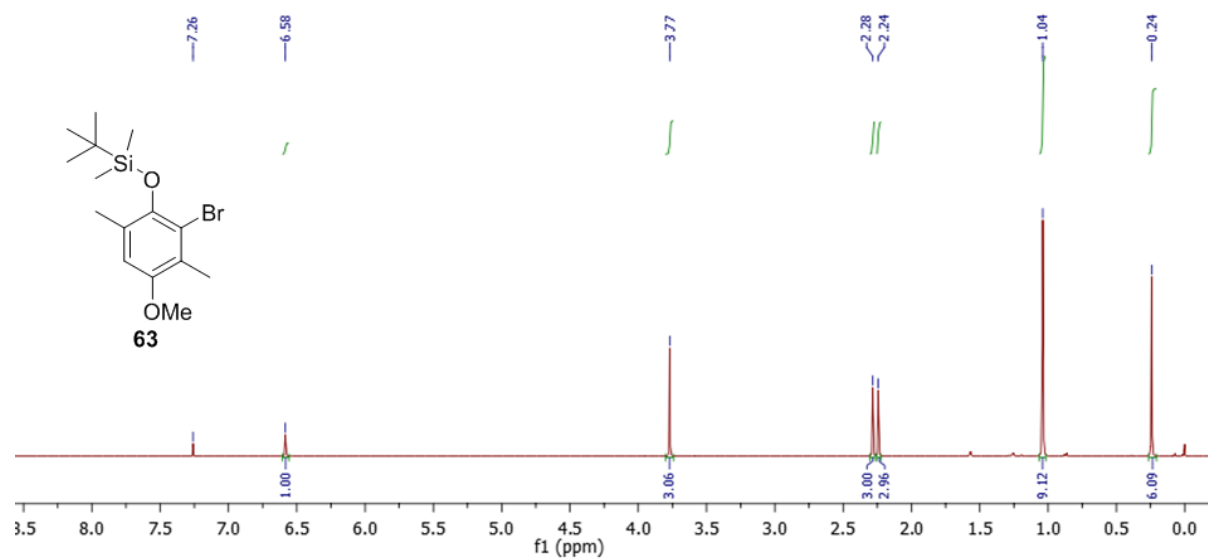
^1H spectrum of **62** (CDCl_3 , RT)



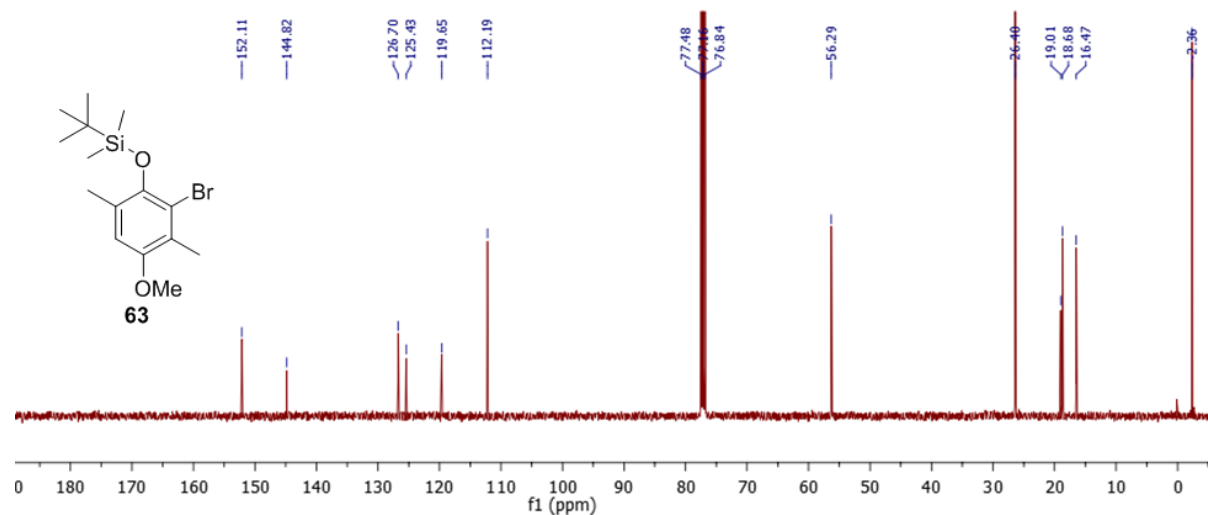
$^{13}\text{C}\{^1\text{H}\}$ spectrum of **62** (CDCl_3 , RT)



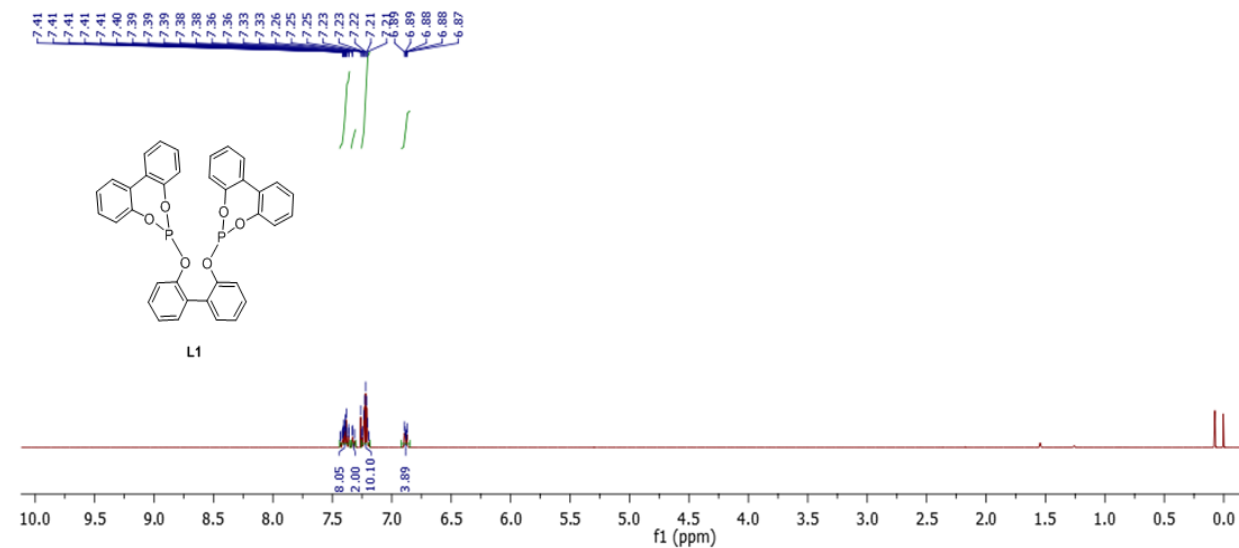
^1H spectrum of **63** (CDCl_3 , RT)



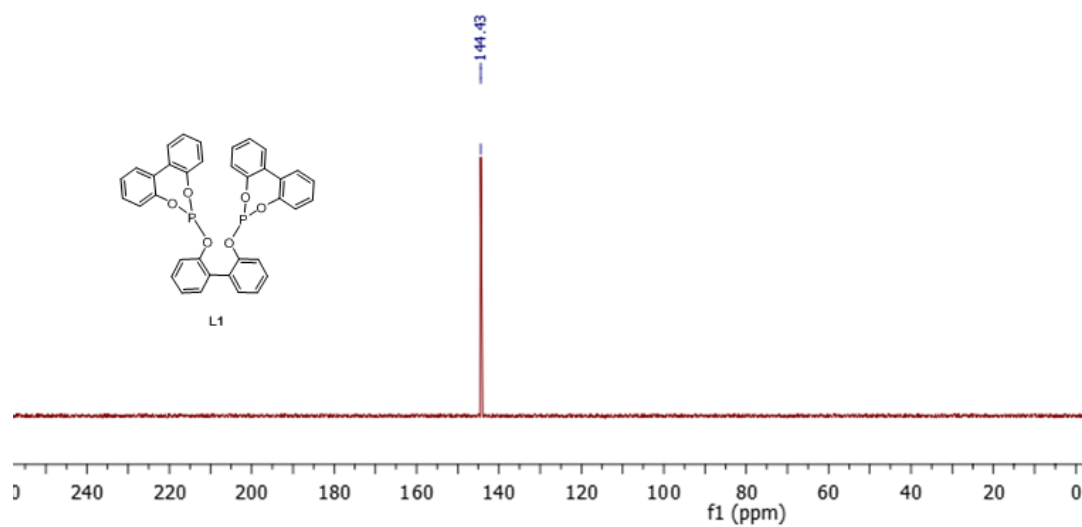
$^{13}\text{C}\{^1\text{H}\}$ spectrum of **63** (CDCl_3 , RT)



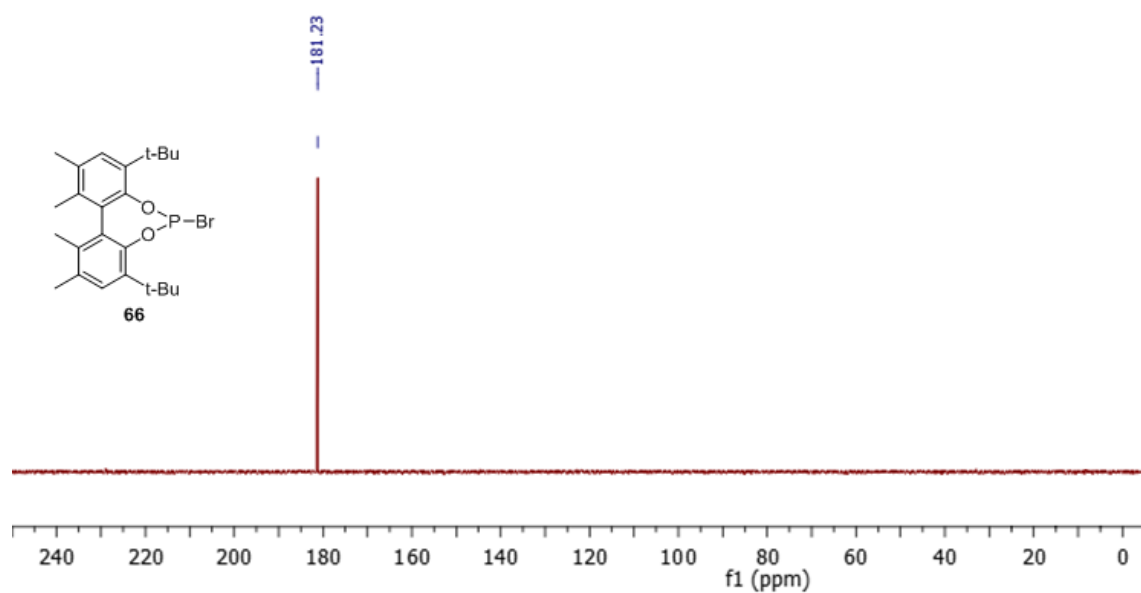
^1H spectrum of **L1** (CDCl_3 , RT)



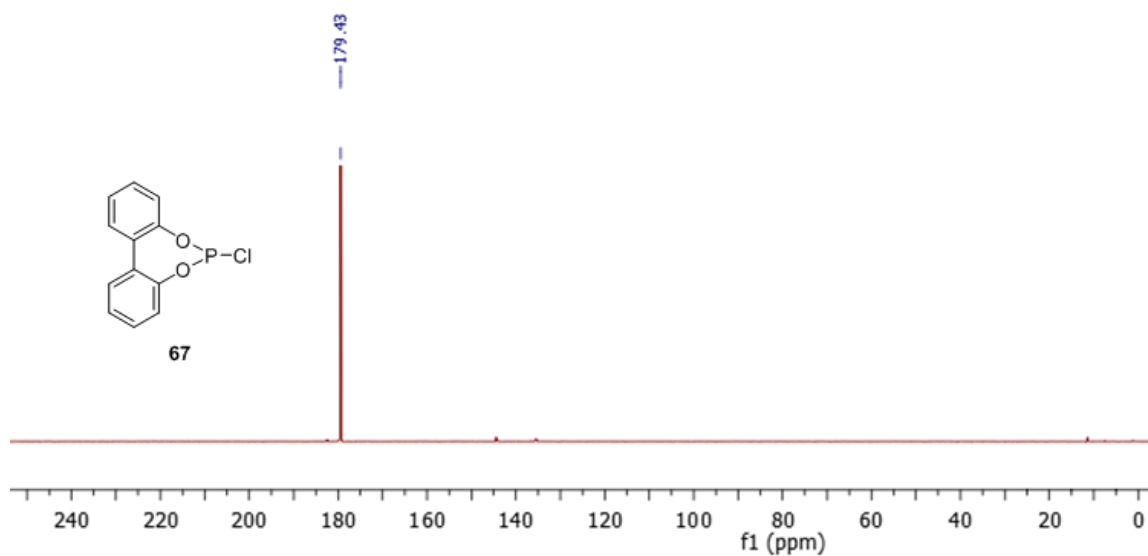
$^{-31}\text{P}\{^1\text{H}\}$ spectrum of **L1** (CDCl_3 , RT)



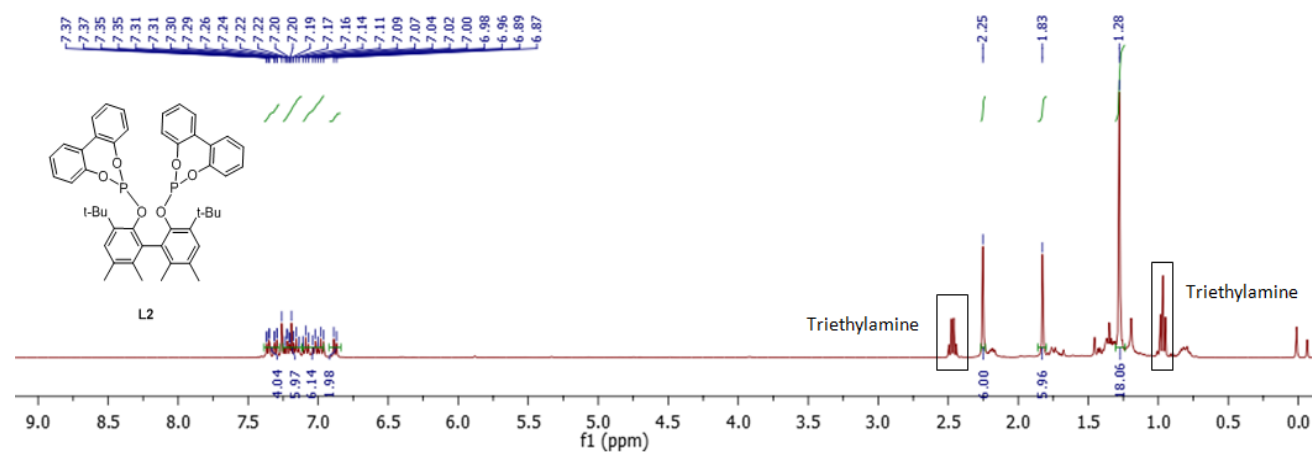
$^{-31}\text{P}\{^1\text{H}\}$ spectrum of **66** (toluene- d_6 , RT)



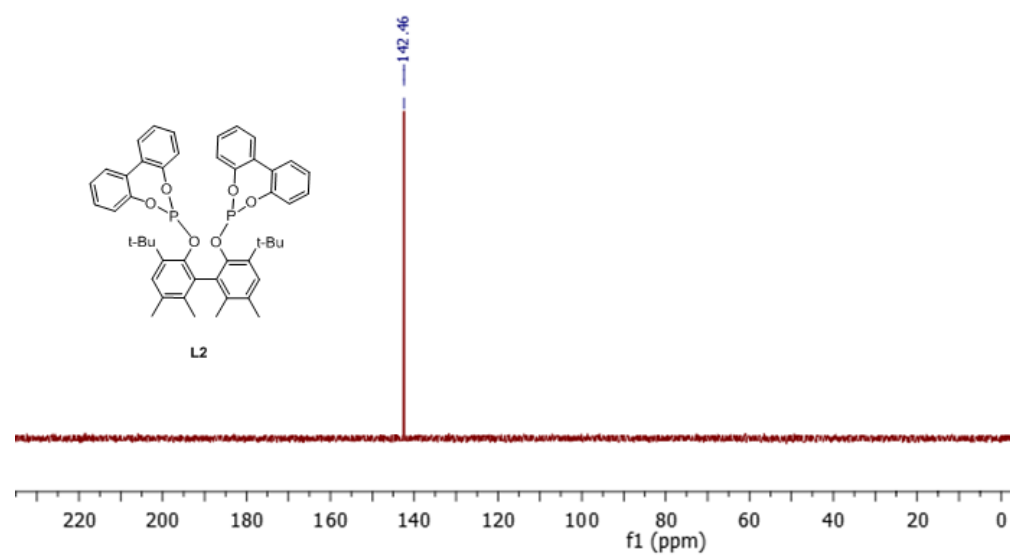
$^{-31}\text{P}\{^1\text{H}\}$ spectrum of **67** (toluene- d_6 , RT)



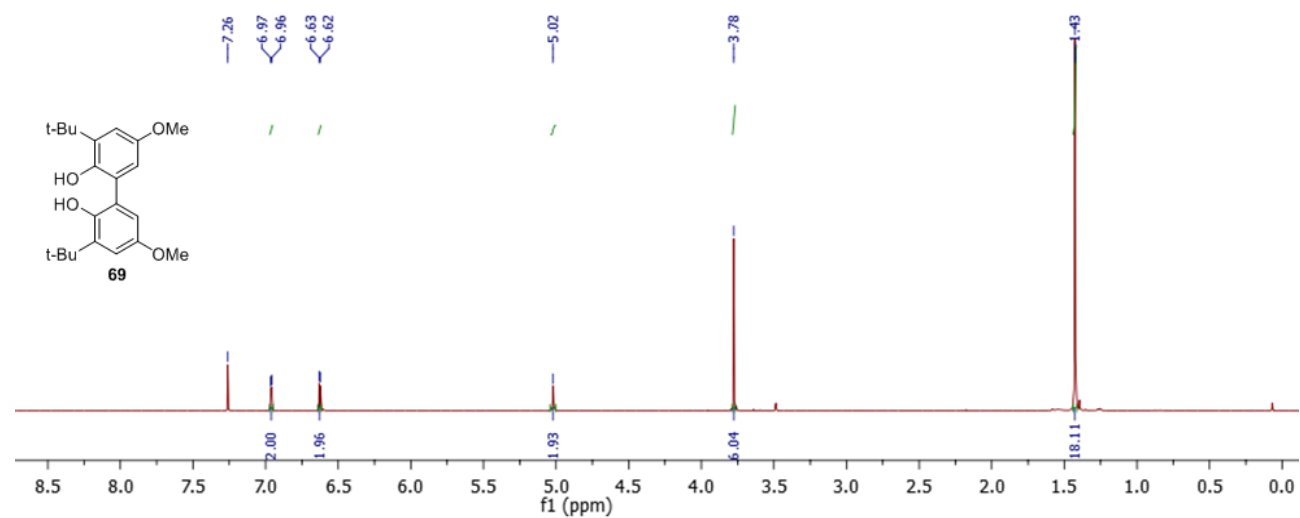
^1H spectrum of **L2** (CDCl_3 , RT)



$^{31}\text{P}\{^1\text{H}\}$ spectrum of **L2** (CDCl_3 , RT)



^1H spectrum of **69** (CDCl_3 , RT)



$^{-31}\text{P}\{^1\text{H}\}$ spectrum of **70** (toluene- d_8 , RT)

